Development of GeoDatabase for the Inner Bay of Fundy: Mapping mudflats and salt marsh Pre and Post Dykes

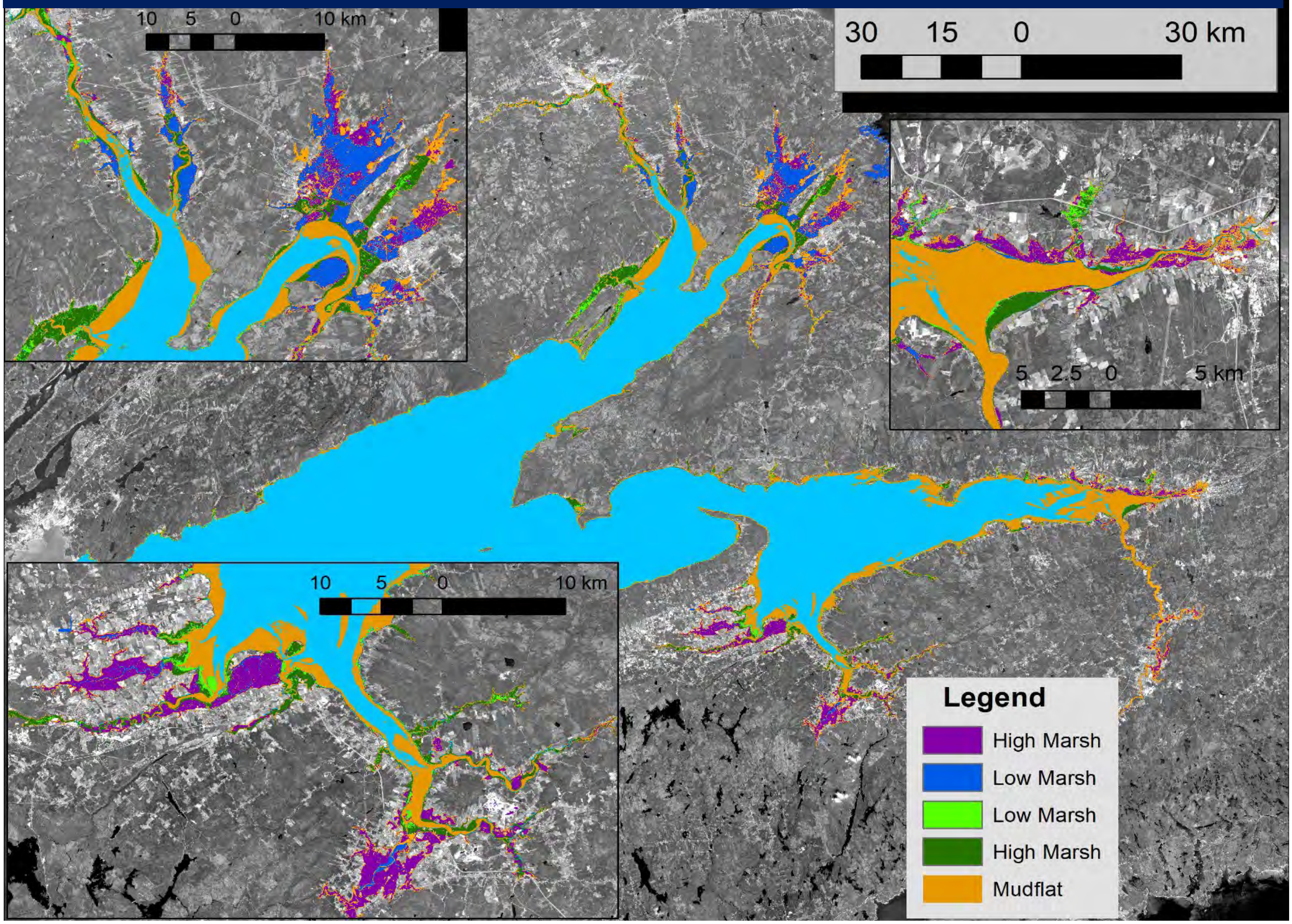

Prepared by

Applied Geomatics Research Group
NSCC, Middleton
Tel. 902 825 5475
email: tim.webster@nscc.ca

Submitted to

Karel Allard, PhD
Marine Conservation Partnerships
Coordinator, Protected Areas
Canadian Wildlife Service
Environment and Climate Change Canada
Government of Canada
March 31, 2022

How to cite this work and report:

Webster, T., McGuigan, K. Roscoe, M., Douglas, L. 2022. Development of GeoDatabase for the Inner Bay of Fundy: Mapping mudflats and salt marsh Pre and Post Dykes. Technical report, Applied Geomatics Research Group, NSCC Middleton, NS.

Copyright and Acknowledgement

Executive Summary

Researchers from NSCC-AGRG and the Canadian Wildlife Service have partnered to construct a high-resolution GIS database of features in the Inner Bay of Fundy. GIS analysis was conducted to address the following questions: map the head of tide of the major rivers and map the extend of mudflats and salt marshes pre and post dyke construction. Additional information related to the proximity of threats to these ecosystems were also implements. Both NB and NS are now fully covered with topographic lidar and form the foundation of some of the analysis. In the case of NS much of the coastal area was surveyed at low tide, thus allowing the mudflat and salt marsh elevations to be captured. To calculate the head of tide for the major rivers, Higher High Water Large Tide (HHWLT) from the Canadian Hydrographic Service was used to relate to the CGVD2013 vertical datum of the lidar data. The HHWLT ranges from 3.9 m near Digby to 7.2 m in the Minas Basin, to 7.5 m in Truro and 6.7 m in the Tantramar area. The HHWLT data were queried for each river and elevations were then applied to the lidar data to calculate the head of tide location. The inner bay was split into sections based on the HHWLT range and coastal flood inundation maps were constructed for present day and 2100 considering RSL. The inter tidal mudflats and salt marshes were extracted using Google Earth Engine where 880 Sentinel-2 images at 10 m resolution were used. The amount of mudflat that could have existed before the dykes were built was estimated by calculating the area landward of the dykes that was connected and below the HHWLT elevation. For the salt marshes, elevation statistics were calculated for the low and high marsh for each of the 5 regions from the lidar DEMs. The mean plus and minus 1 standard deviation was used to calculate elevation thresholds for the low and high marsh, which were modified to ensure no overlap between boundaries and did not exceed the HHWLT elevation. The lidar data landward of the dykes were then modelled based on these salt marsh elevation threshold values to predict where low and high marsh could grow. Analysis indicates that approximately 40% of mudflats and 66% of salt marsh has been lost as a result of dyking.

Table of Contents

Table of Figures

List of Tables

1 Introduction

The objective of this project was to enable Inner Bay of Fundy (IBoF) planning team access to best-available foundational baseline information to consider in designing, delineating and implementing effective conservation measures (i.e. strategies). The background and specific scope of the requirement for this project is the recognized importance of the Inner Bay of Fundy for a broad range of ecosystem and human well-being values and the significance of legacy, ongoing and emerging land- and marine- based pressures on the marine environment. The functional spatial scope of the Inner Bay of Fundy Initiative includes waters of the IBoF to head of tide, though its practical scope transcends the marine-terrestrial divide. Its outside limit is to a line intersecting the Bay of Fundy from Cape Spencer Lighthouse to Digby Gut Lighthouse and is generally reflective of the seaward extent of the Siknikt District (Figure 1).

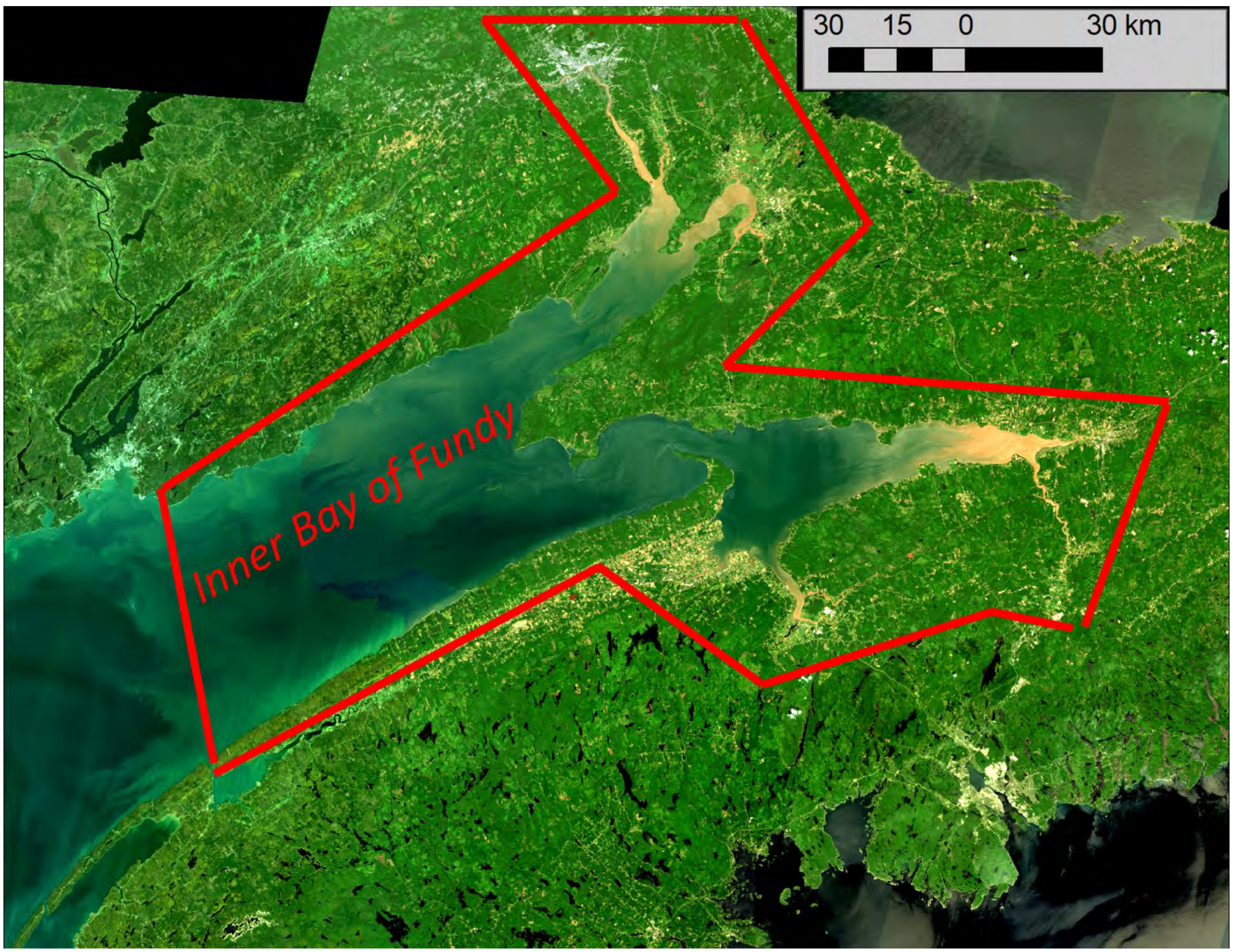

Figure 1 Study area of the Inner Bay of Fundy (IBoF). Background image is a 10 m true colour Sentinal-2 image mosaic.

Topographic lidar has been acquired by both principal governments from NB and NS that borders the IBoF. Topo lidar works by emitting a near-infrared (NIR) laser pulse from an aircraft and measuring the travel time of the laser pulse to and from the land or water surface or features on the land. The end result of a lidar survey is a 3-D point cloud of elevations. This point cloud is then examined, and the points are classified based on what they represent. The data for NS and NB is simply classified as ground and non-ground. From the ground only points a Digital Elevation Model (DEM) is constructed that represents the bare earth. In the case of NS, the lidar provider was instructed to collect the data within 2-3 hrs of low tide, thus ensuring the elevation of the intertidal areas would be captured. Unfortunately, this was not the case for NB and the lidar is not sufficient to provide elevation details along the IBoF coast for much of NB. However, these data were critical in constructing some of the layers requested for this IBoF initiative (Figure 2).

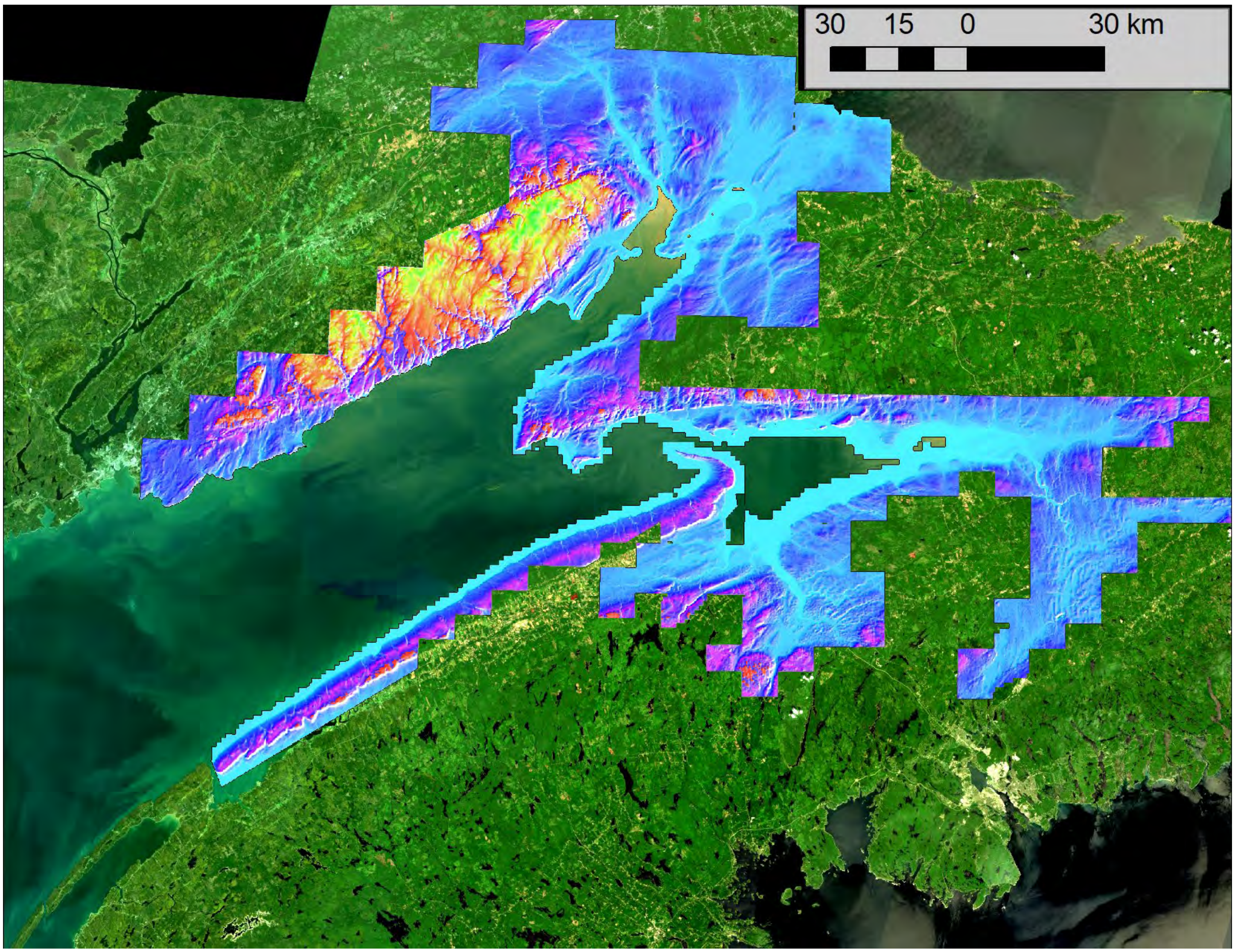

Figure 2 Inner Bay of Fundy with shaded relief topographic lidar DEM around the boarder.

The initiative set forth a set of geographic representations of various factors that are considered important for the IBoF. Many of these GIS layers do not exist and needed to be constructed using the best available methods and data at the time. A list of items include:

- Include tidally influenced portions of rivers (Riverine Estuaries), using the best available (i.e. standardized) decision rule to determine ordinary head of tide
- Include best-available delineation of OHW to establish landward extent of scope
- Include predicted year 2100 sea-level rise extent as secondary scope geography, using static (i.e. bathtub) model (i.e. with and without anthropogenic dykes and water control structures; see component 2)
- Include CPCAD layer of terrestrial Protected and Conserved Areas
- Include delineation of IBoF watersheds
- Calculate “Saltmarsh extent” – Total area (ha) under two scenarios: present-day and historical coastline (i.e. prior to dyking). For former, use best available decision rule (e.g. using imagery) to delineate high marsh vegetation versus low marsh vegetation, and calculate extent of each.
- Incorporate various GIS layers (approximately 20 layers) that exist with other government departments and ENGO’s used to characterize (i.e. spatial extent, severity) those pressures/threats outlined in “Pressures Table”, in IBoF Workshop Report 2021.pdf. CWS-ECCC will facilitate the data transfer to NSCC-AGRG.
- For each conservation target, assess target health through calculation of all KEA indicators requiring GIS. For example, using present-day coastline calculate “Amount of undisturbed saltmarsh” - % of saltmarsh outside 100 m or disturbance. Disturbance here defined as: Roads, Buildings, Shoreline hardening, Dykes, Infilling and other development.

Specific deliverables for the first year of this 2-year study included:

1. Bay of Fundy scope layer map; present-day saltmarsh extent; present-day mudflat extent; seamless land-sea LiDAR elevation model for the Inner Bay of Fundy and adjacent watersheds.
2. Calculated values for marine target Key Ecological Attributes and associated target health indicators, as per IBoF Workshop Report.
3. Bay of Fundy scope layer map; historical pre-settler saltmarsh extent.
4. Present best-available spatial layers to characterize present-day extent of anthropogenic threats/pressures, as per IBoF Workshop Report, as identified by and obtained from IBoF Initiative team members.
5. Design and architecture of robust Arc Geodatabase shareable among IBoF Initiative team members (to federal Geospatial Metadata Standard). First iteration.

As mentioned, many of these datasets did not exist with any government or organizations. Thus, a series of GIS and image processing analytical techniques were undertaken to construct these layers. The methods section will describe the various datasets used and the analysis techniques to derive some of these requested layers.

2 Methods

2.1 Higher High Water Large Tide

Any of the geospatial layers requested by the IBoF initiative were related to the extent of high tide. The large tidal range in the IBoF along with the ample supply of sediment gives rise to the extensive mudflats and salt marshes that are associated with this unique place and what makes it critical to so many migrating birds along their migration path. The Canadian Hydrographic Service (CHS), part of Department of Fisheries and Oceans (DFO) are responsible for measuring and predicting the tides along Canada's coasts. In 2010, CHS in collaboration with Canadian Geodetic Survey (CGS) began development of the Continuous Vertical Datum for Canadian Waters project (CVDCW). The goal was to develop a surface connecting chart datum (CD) to the national geodetic reference frame which captures the relevant spatial variability as modeled by integrating ocean models, water levels, GPS observations, sea level trends, satellite altimetry, and a geoid model. Other surfaces included in the effort (e.g. low water, high water) provide fundamental pieces of information for coastal studies, climate change adaptation, and the definition of the Canadian shoreline and offshore boundaries (Robin et al., 2014).

The CVDCW was obtained through CHS for Atlantic Canada and consists of a series of points spaced at ~ 100 m along the coast (Figure 3).

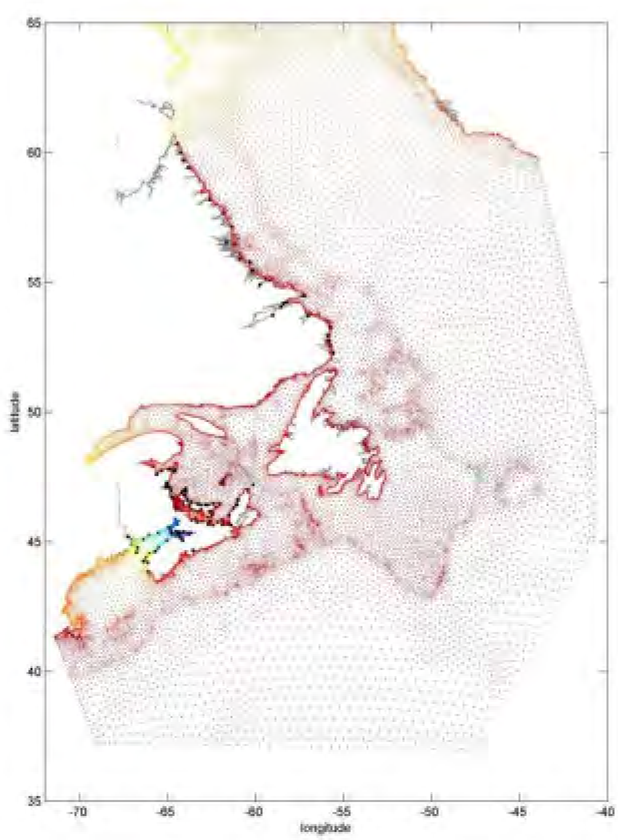

Figure 3 Example of the CVDCW for Atlantic Canada. Source Phillip MacAulay, CHS-DFO.

There are several files that can be used that related the elevation of CD as well Higher High Water Large Tide (HHWLT), defined as the average of the yearly predicted water level maximums from a 19-year astronomical cycle (i.e. the average of 19 predicted values), Mean Water level (MWL) and Lower Low Water Large Tide (LLWLT), defined as the average of the yearly predicted water level minimums from a 19-year astronomical cycle (i.e. the average of 19 predicted values), to the most current vertical datum, the Canadian Geodetic Vertical Datum 2013 (CGVD2013). In the figure below the various water level surfaces are referenced along with Chart Datum (CD) and the older Canadian Geodetic Vertical Datum 1928 (CGVD28) (Figure 4).

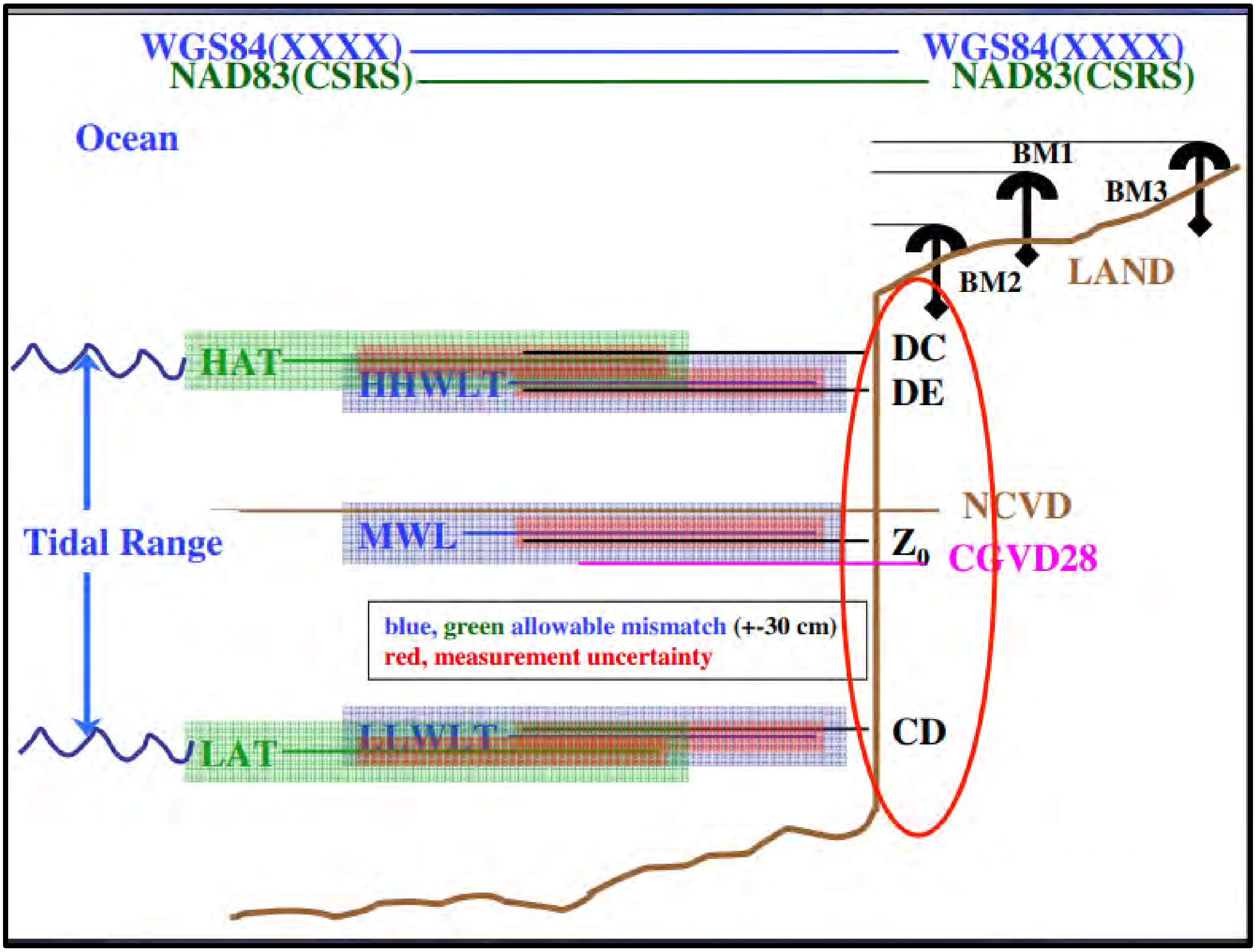

Figure 4 Example of various tidal water surfaces (e.g. HHWLT) relative to vertcial datum (e.g. CD and VGVD28). Source Phillip MacAulay, CHS-DFO.

There is no vertical information along the coast for Ordinary High Tide, however there is for the larger tides HHWLT which is defined in the CVDCW. There is a significant variation in the elevation of the HHWLT as one moves inward along the IBoF where the highest elevations are reached in Cobequid Bay near Truro, NS (Figure 5). Appendix 1 shows the relationship of HHWLT to the regular tide for three sites within the IBoF.

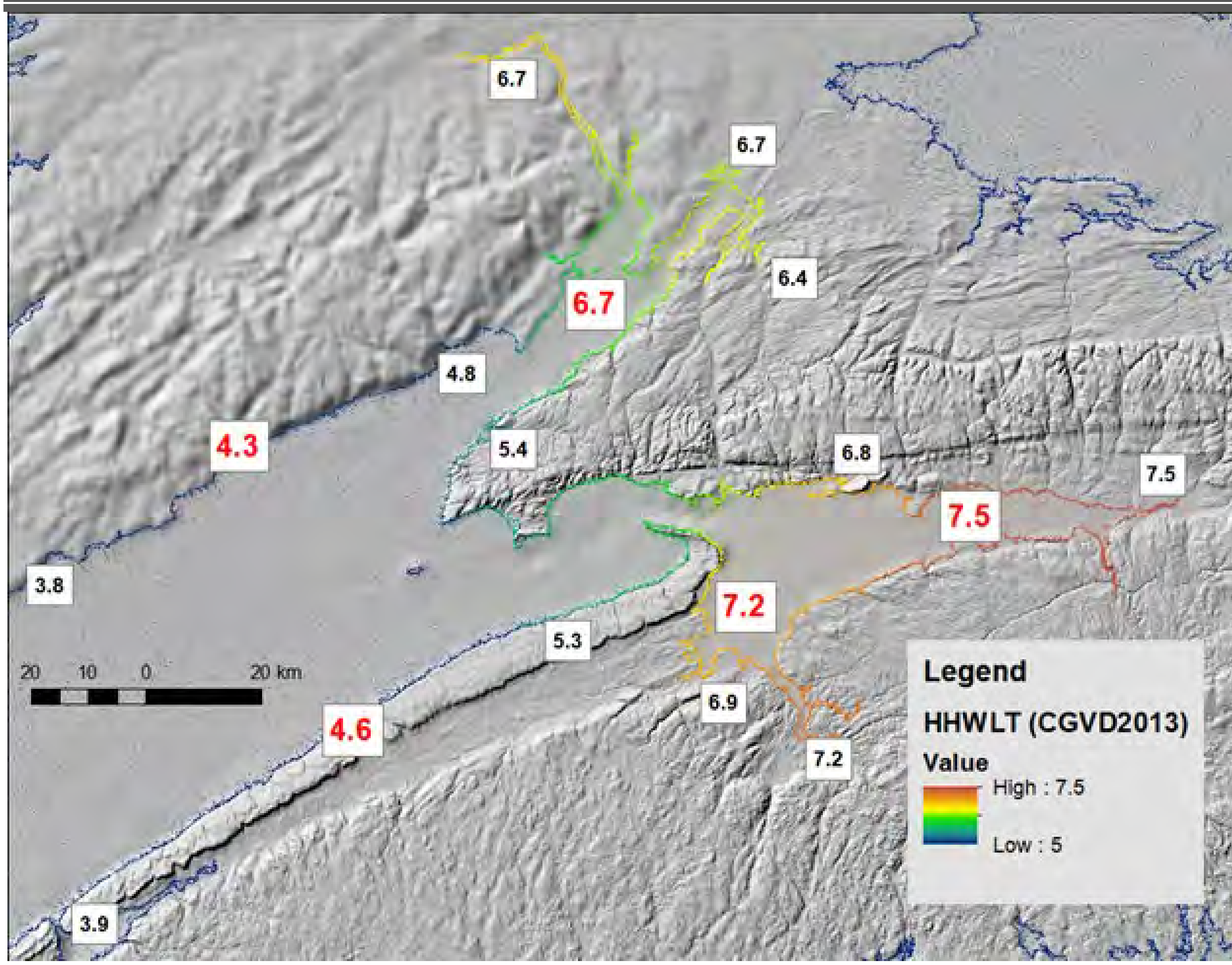

Figure 5 The CHS CVDCW data gridded at 100 m and select values highlighted showing the elevation in CGVD2013 for the HHWLT.

In figure 5 the grid is colour coded based on the CGVD2013 height of HHWLT and specific sites are shown in black numbers for different areas around the IBoF. Since there is a significant variation in the elevation of HHWLT around the IBoF, the bathtub model approach of sea level rise on top of HHWLT from storm surge or long-term climate change is not feasible for the entire bay. As a result of this condition, the IBoF was separated into five regions for sea level rise analysis and coastal mapping. The five regions were based on their HHWLT range and consisted of: Cobequid Bay, Minas Basin, Chignecto Basin, NB Bay of Fundy Coast, and the NS Bay of Fundy Coast. The large red numbers in figure 5 denote the HHWLT used for each one of these sights. The lidar data from the provinces were split into these five regions and used to develop the HHWLT maps and the flood risk maps (Figure 6). For the head of tide mapping for the major rivers draining into the IBoF, the lidar was use explicitly for each river and a specific HHWLT value was used. In many areas of the IBoF dykes protect low lying areas landward of the dyke. The projection of HHWLT elevations on the lidar from the five regions in the IBoF (Figure 6) denotes the current extent of the ocean onto the land. For each of the five regions, the projected water level (HHWLT) was used to map the extent and then only areas that were connected to the Bay of Fundy were selected. In other words, only areas seaward of the dykes were selected from the HHWLT extent. If these dykes were removed or were never built, the projection of HHWLT would depict how far the ocean would extend landward.

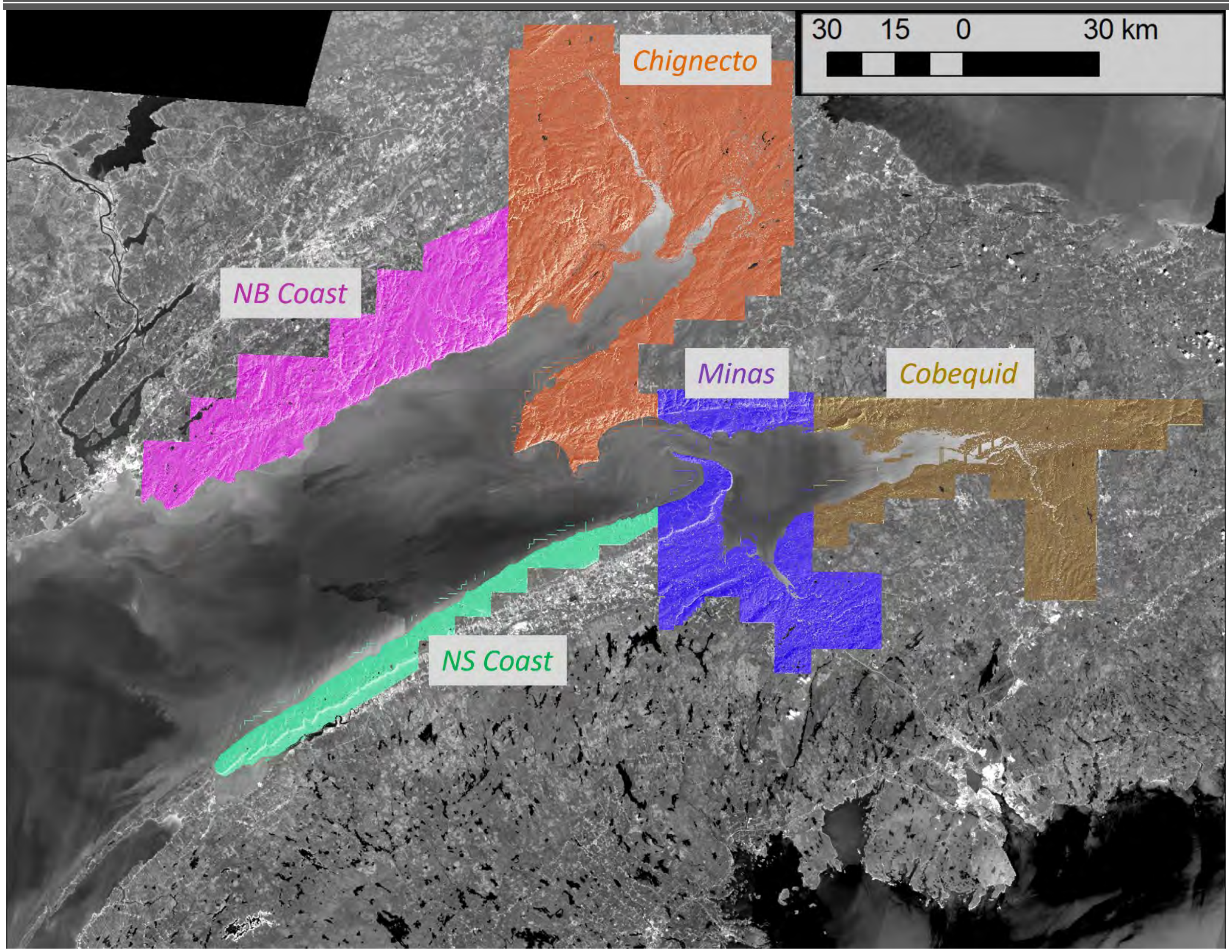

Figure 6 Location of the 5 regions and lidar data of IBoF: Cobequid, Minas, Chignecto, NB Coast and NS Coast.

As mentioned, we have constructed "Head of Tide" maps for all the major rivers draining into the IBoF. In that analysis the HHWLT was queried for every river and the lidar was clipped and used to construct the extent of head of tide. Extreme care was taken to assess the drainage characteristics of each river and weather it was controlled by an aboiteaux or not.

2.2 IBoF Shoreline today and in 2100

To map the present-day shoreline, we projected the HHWLT elevation on each of the five lidar regions (Figure 5, Table 1). These flood levels also included low lying areas behind the dykes (Figure 7). Therefore, only areas that were connected to the Bay of Fundy were selected from this map and used to construct the present day shoreline for the IBoF (Figure 8).

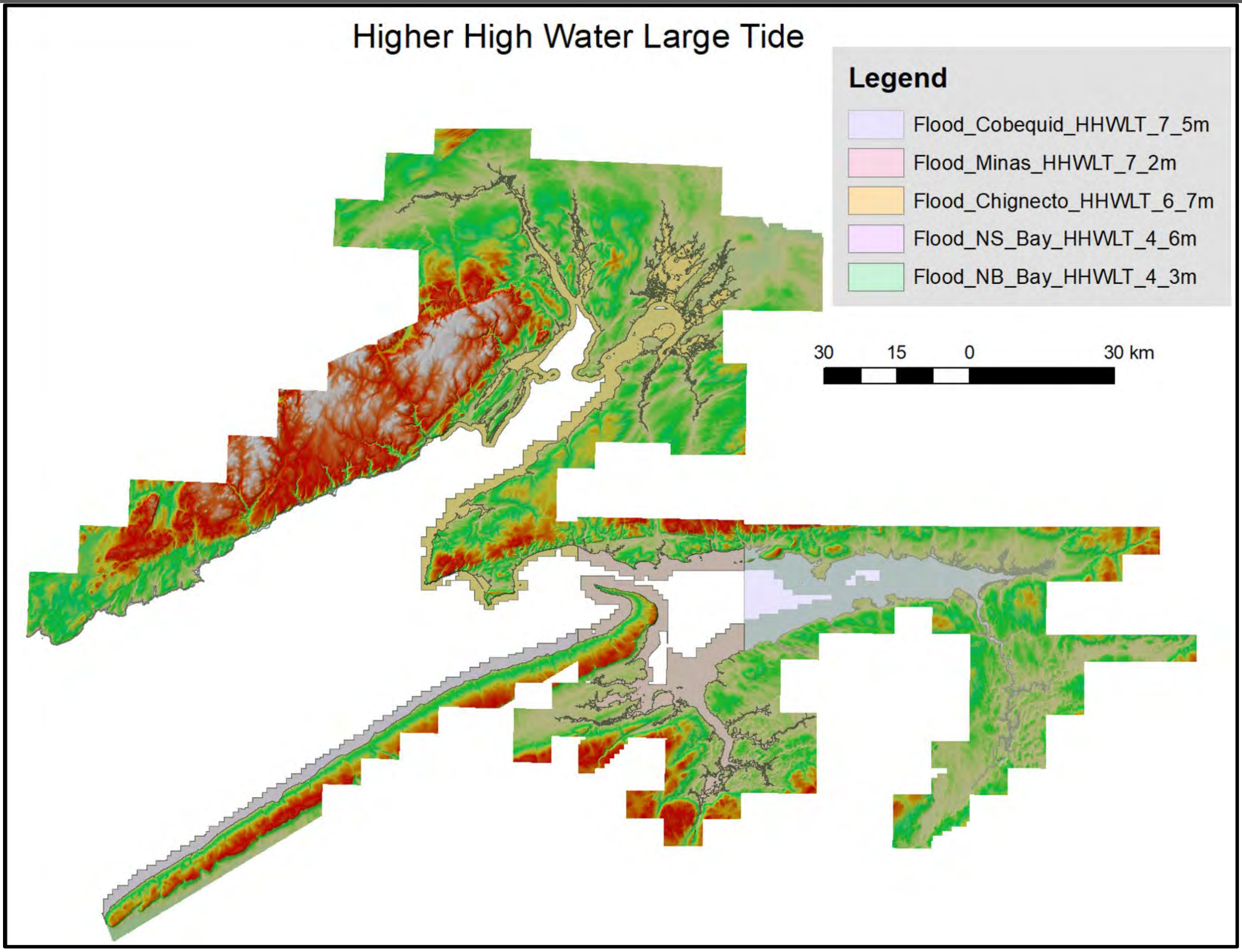

Figure 7 Map of HHWLT for IBoF. These polygons also include low lying areas behind protective dykes.

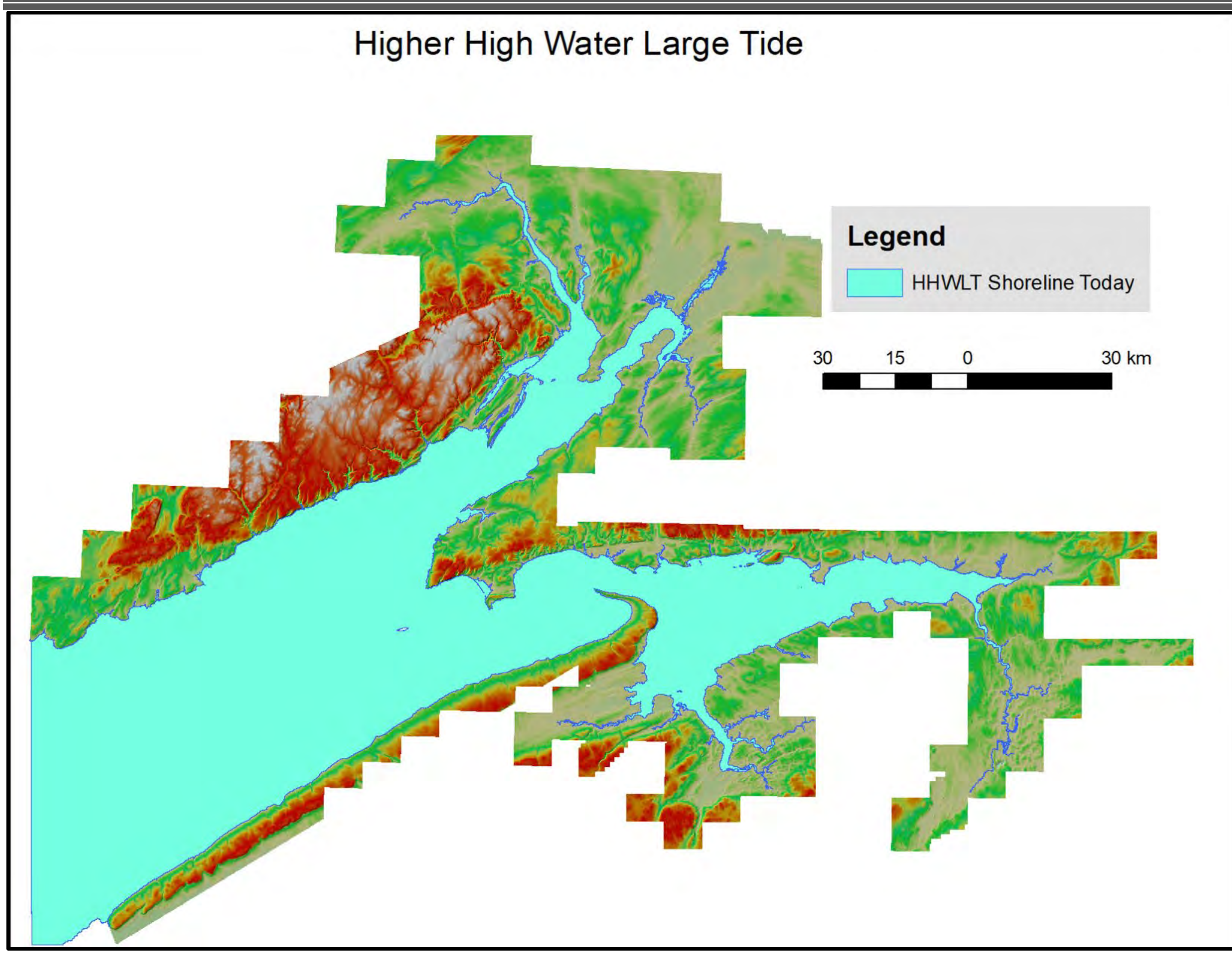

Figure 8 Present day shoreline of IBoF (HHWLT).

Based on the predictions of relative sea level rise (RSL) we can also predicted what the shoreline will look like in 2100. The RSL takes into account both global sea level rise and crustal subsidence and is depicted in Table 1.

Basin	HHWLT (m GVD2013) Head of Tide	1:100 yr Storm Surge (m)	Present Day Flood Level (HHWLT + 1:100 Storm Surge)	Relative SLR by 2100 (m) (SLR, crustal adj., Antarctic ice collapse, 10 cm Tidal Expanse)	2100 Flood Level (HHWLT +1:100 Storm Surge + RSL, 10 cm Tidal Expanse)
Cobequid	7.5	1.2	8.7	1.8	10.5
Minas	7.2	1.1	8.3	1.85	10.2
Chignecto	6.7	1.2	7.9	1.8	9.7
NB Coast	4.3	0.8	5.1	1.9	7.0
NS Coast	4.6	0.8	5.4	1.8	7.2

Table 1 Water levels for the five regions in the IBoF. Includes present day flood level as well as the predicted water level in 2100. Adapted from van Proosdij et al. (2018) and Richards and Daigle (2011).

The shoreline in 2100 was calculated by using the HHWLT for the five regions and then adding RSL values to the HHWLT elevation for each region and then combining them (Table 1). Additional factors considered in RSL for 2100 also include a possible tidal expansion of up to 10 cm (Greenburg et al., 2012) with global SLR and the collapse of the western Antarctic ice sheet, estimated to add 65 cm (IPCC, 2013; James et al. 2014). With RSL added to HHWLT the Bay of Fundy actually connects to the Northumberland Strait, thus making NS an island (Figure 9). When examined in detail, there is a very small connection between the IBoF and the Northumberland Strait at a wetland between the two.

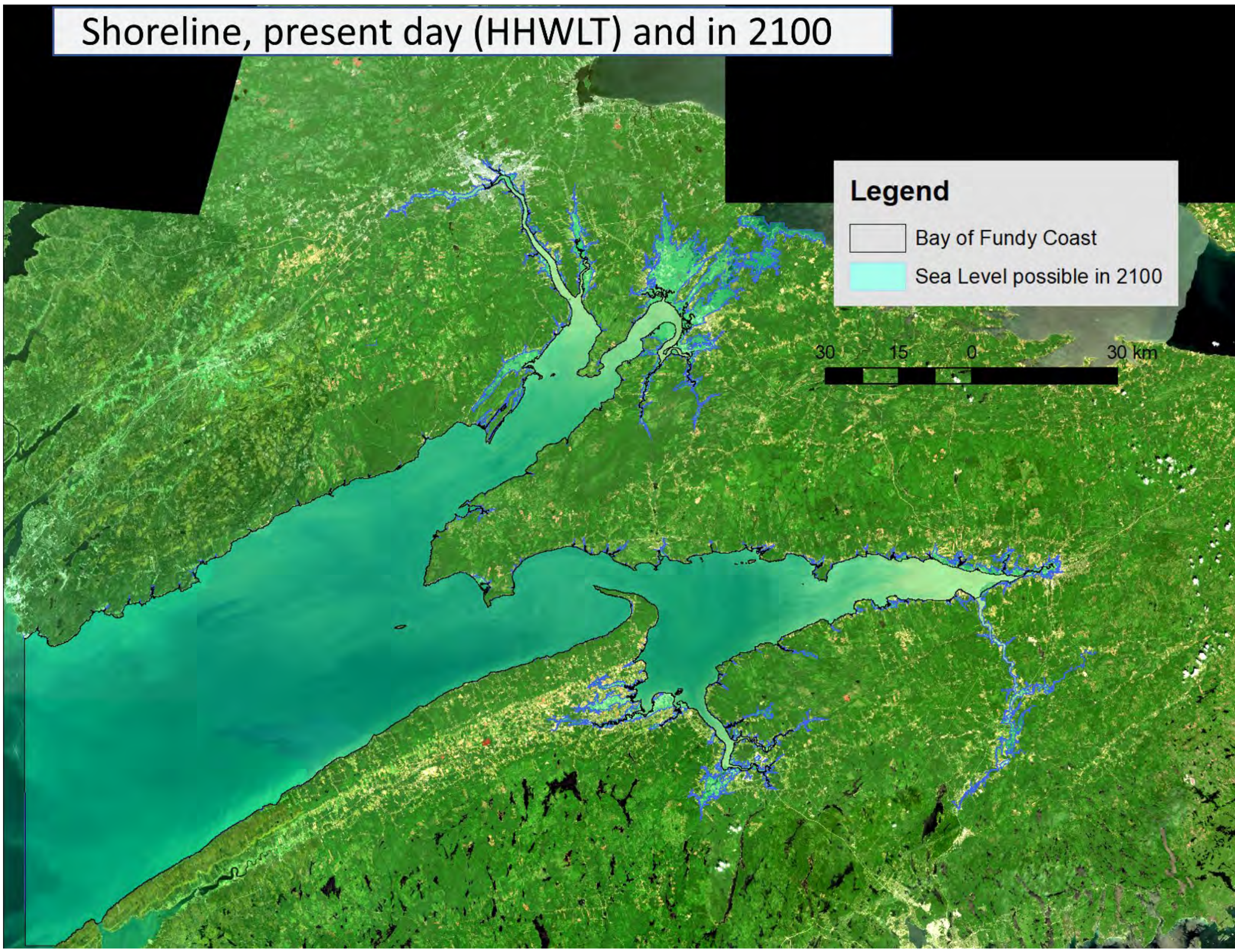

Figure 9 Present day shoreline (HHWLT) and the predicted shoreline in 2100 considering RSL rise.

2.3 Coastal Flooding today and in 2100

To calculate the present-day coastal flood risk and what it would be in 2100 considering climate change impacts, the five regions were analyzed separately and then the results were combined. The assessment of flood risk was based on using the proposed standard from NS which suggests using the HHWLT elevation plus the 100-year return period storm surge value. For flood risk in 2100 we consider relative sea level rise (RSL), which includes global seal level rise, crustal subsidence, tidal expansion within the bay and the collapse of the western Antarctic ice sheet. The elevations for the present-day and predicted 2100 water levels are presented in Table 1 for the five regions. To generate the present-day flooding, the lidar for each of the five regions was used with the bathtub model approach to map the Present-Day Flood Level (Table 1). During this process at the initial flood stage, low lying areas behind the dykes are also flooded. At step two of the process, only the areas that are connected to the ocean are selected and included in the mapping. This same process was followed for the 2100 flood levels.

We also constructed flood layers for the present-day and in 2100 assuming there were no dykes or barriers to flow. Only a few isolated polygons needed to be removed during the inspection of the flood polygons resulting from this analysis.

2.4 Head of Tide for Major Rivers in IBOF

For each major river the CVDCW HHWLT value furthest inland was used to establish the head of tide elevation. Using Lidar elevation models for each major river, a binary 1-meter resolution raster made showing the extent of the head of tide based on the HHWLT elevation. The head of tide rasters were then polygonised to create the head of tide polygon shapefiles for each river. By selecting the head of tide polygon directly connected to the ocean and exporting selected features the head of tide polygon shapefiles were constructed. In some instances, modifying the connected head of tide polygons was necessary to include dams and aboiteaus. Structures such as dams and aboiteaus were located using government data when available and interpreted from satellite imagery when no government data was available. A larger list of dams and aboiteaus in Nova Scotia which are part of the Working with the Tides project is available at the NS government site (https://novascotia.ca/dykeland-system-upgrades/dykeland-sites/). Two layers were produced as a result. The head of tide polygon layers which show all areas which are connected to the ocean and another layer that is landward but not connected to the ocean. With the connected head of tide polygon overlayed on the head of tide polygon you can visualize the areas which are disconnected from head of tide, such as dykelands and other low-lying areas not directly connected to tidal influence. A total of 48 rivers were used to calculate the head of tide (Table 1). Examples of Peticodiac and Memramcook rivers shows the effects of dyking and flow control structures such as aboiteaus (Figure 10, Figure 11, Figure 12). Care was taken to ensure the control structure were correct. For example, the Peticodiac River used to be controlled by an aboideaux in Moncton, which has since been removed, thus allowing the head of tide to migrate further in-land than in the past.

River Name	HHWLT CGVD 2013 (m)	River Name	HHWLT CGVD 2013 (m)	River Name	HHWLT CGVD 2013 (m)
Mispec River (NB)	3.644	Sheopody River (NB)	5.874	Habitant River (NS)	6.817
Black River (NB)	3.896	Diligent River (NS)	5.911	East River (NS)	6.822
Gardner Creek (NB)	4.015	Shulie River (NS)	6.148	Cornwallis (NS)	6.875
Ten Mile Creek (NB)	4.093	Parrsboro Aboiteau (NS)	6.339	Curry Brook (NS)	6.998
Mosher River (NB)	4.397	Memramcook River (NB)	6.346	Economy River (NS)	7.083
Irish River (NB)	4.456	Carters Brook (NB)	6.360	Walton River (NS)	7.117
Big Salmon River (NB)	4.482	Tantramar River (NB)	6.374	Cogmagun River (NS)	7.154
Little Salmon River (NB)	4.611	Aulac River (NB)	6.382	Kennetcook River (NS)	7.187
Quiddy River (NB)	4.670	Missaguash River (NS)	6.404	St. Croix River (NS)	7.214
Goose Creek (NB)	4.710	LaPlanche River (NS)	6.411	Tennycape River (NS)	7.345
Point Wolfe River (NB)	4.830	Nappan River (NS)	6.442	Portapique River (NS)	7.421
Upper Salmon River (NB)	4.933	Maccan River (NS)	6.452	Great Village River (NS)	7.451
Long Marsh Creek (NB)	5.260	River Hebert (NS)	6.480	Folly River (NS)	7.465
Apple River (NS)	5.431	Moose River (NS)	6.614	Chiganois River (NS)	7.472
Fox River (NS)	5.870	Petitcodiac River (NB)	6.676	Salmon River (NS)	7.478
Sawmill Creek (NB)	5.874	Bass River of Five Islands (NS)	6.794	Shubenacadie River (NS)	7.508

Table 2 List of rivers where head of tide was calculated. Tide height given by HHWLT relative to CGVD2-13.

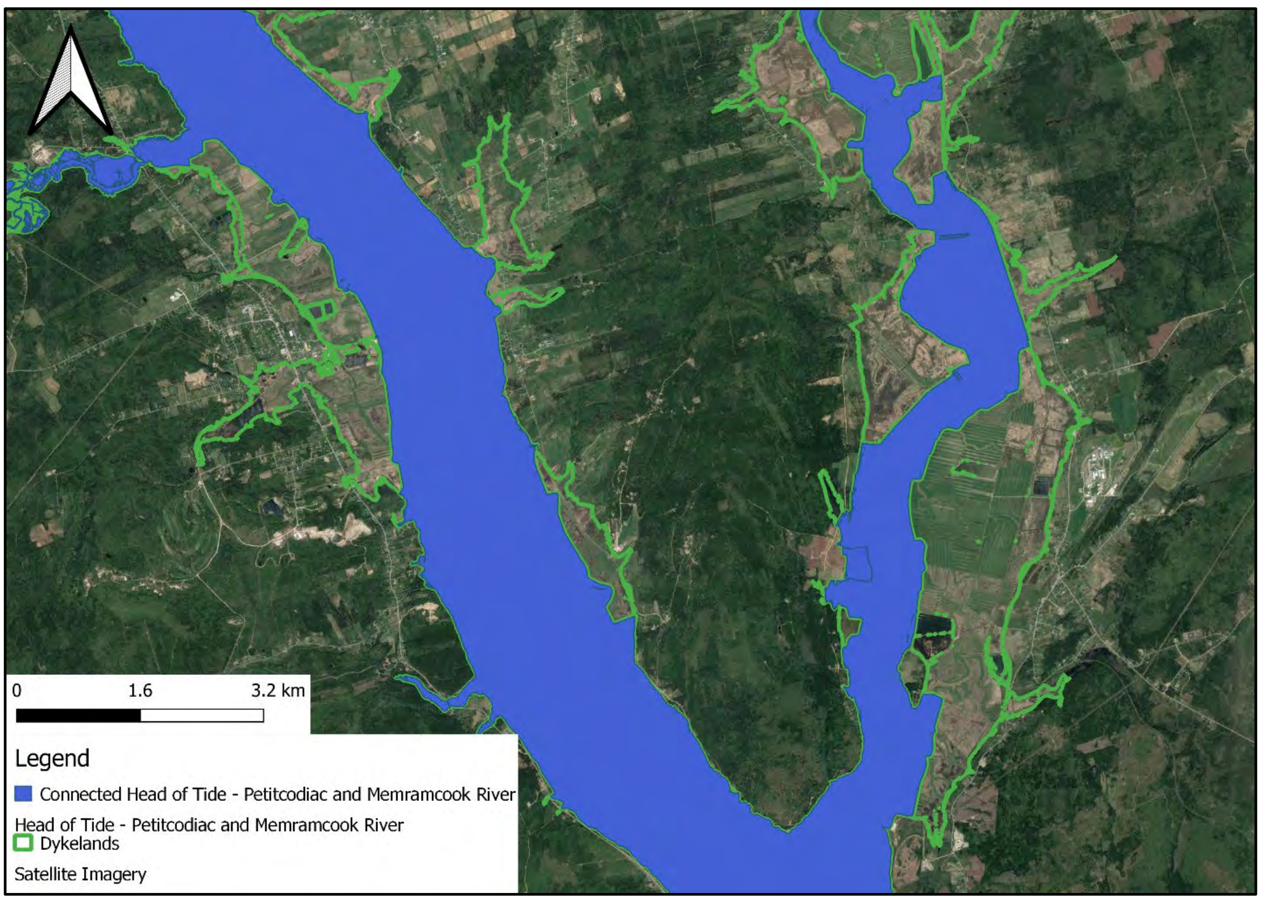

Figure 10 Example of the dykelands where the Peticodiac and Memramcook rivers separate.

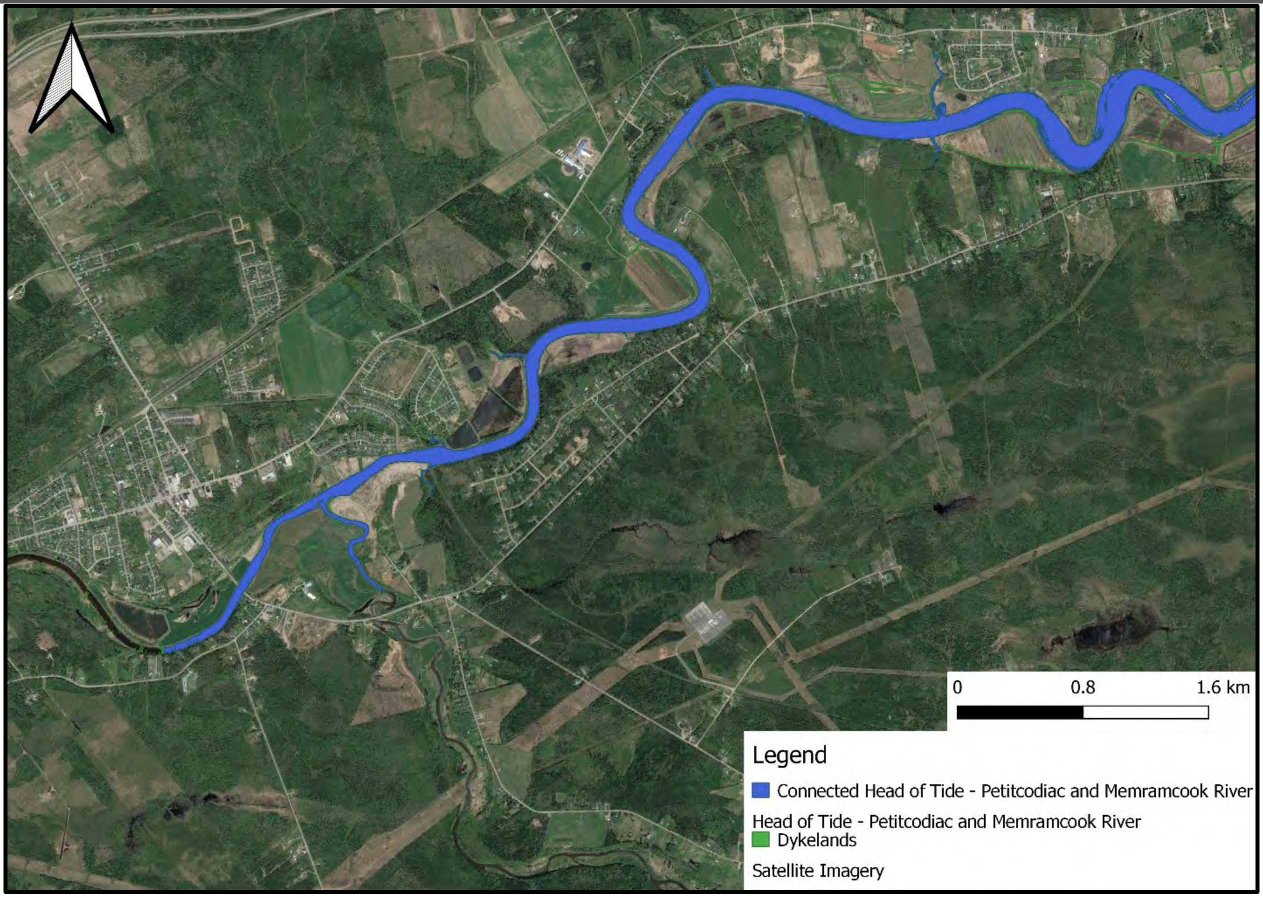

Figure 11 Close-up of Petitcodiac river showing dykelands (green) and connected head of tide (blue) at the furthest reach of head of tide. NOTE: Very minimal dykeland present this far up-river.

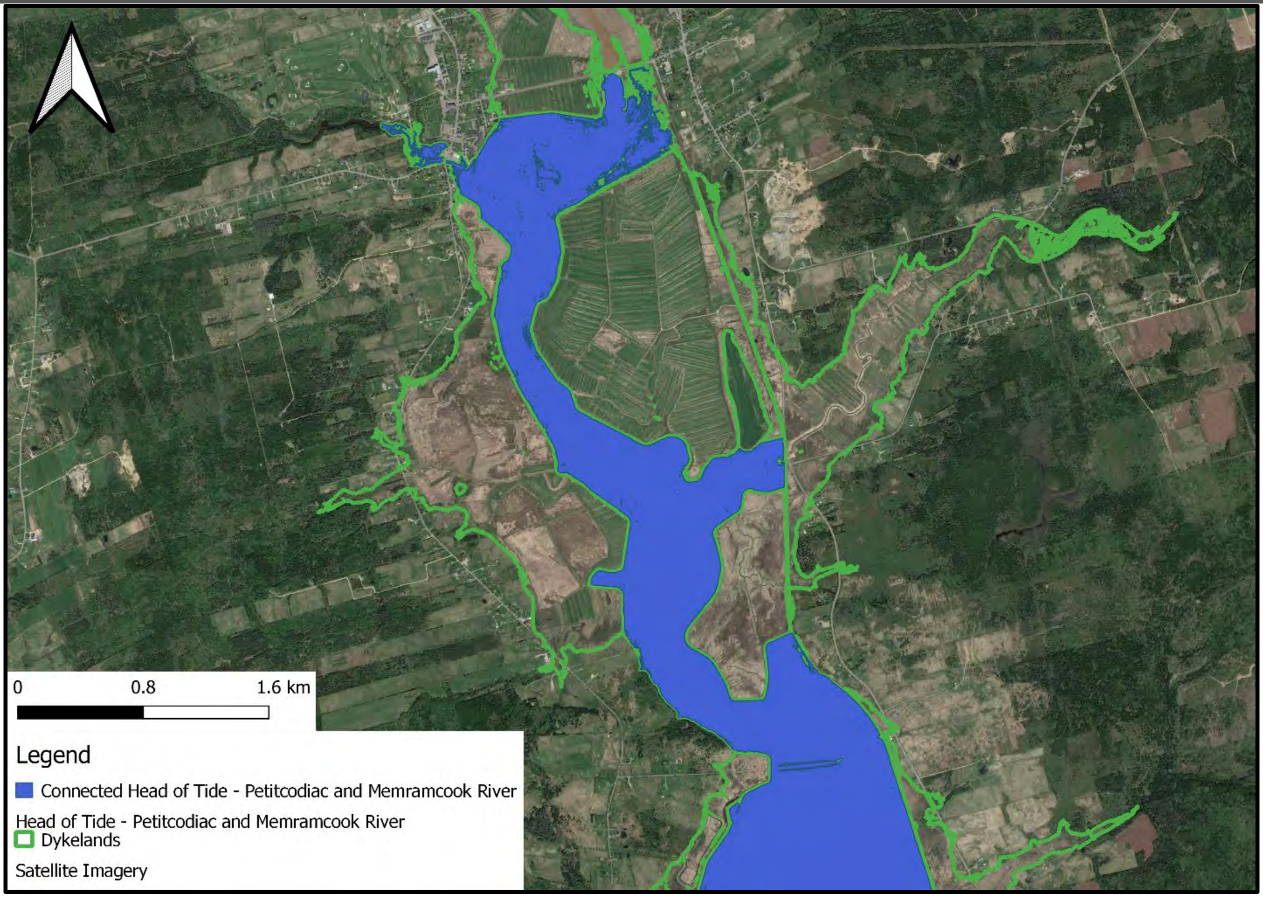

Figure 12 Close-up of Memramcook river showing dykelands (outlined in green) and connected head of tide (blue) at the furthest reach of head of tide.

There are several rivers that have control structure on them that limit the landward extent of the head of tide. For example, the Nappan River has an aboiteau that limits the extent for the head of tide (Figure 13).

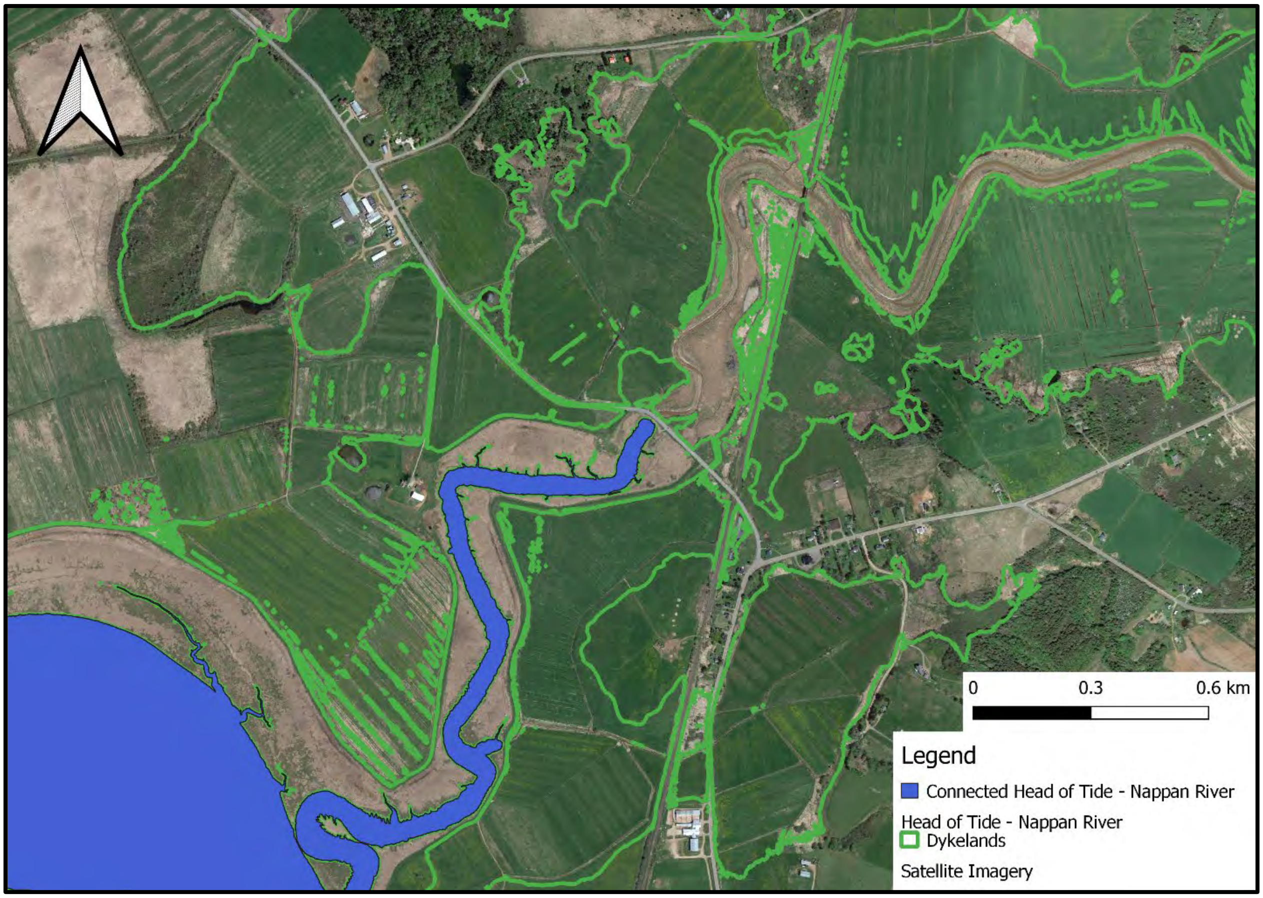

Figure 13 Close-up of the Nappan River at head of tide showing dykelands (outlined in green) and connected head of tide (blue).

2.1 Mapping Tidal Flats & Salt Marsh with Pre and Post Dykes

We were also tasked with mapping the extent of mudflats within the IBoF. We examined the lidar data to determine if we could use it to map the inter tidal mudflats. However, given the variable tidal conditions during the flights and the fact the water was not separated for the land in the coastal zone, the lidar data could not be used to map the mudflats. We also examined a range of satellite imagery and have included several Landsat and Sentinel-2 images in the geodatabase. Landsat imagery has a 30 m resolution while Sentinel-2 imagery for many bands has a 10 m resolution. Examples of the variable tide, mudflat extent and salt marsh vegetation are shown in cloud free imagery for part of Minas Basin (Figure 13).

Based on the fact we needed to use satellite imagery to map the extent of the mudflats and salt marsh communities, we utilized Google Earth Engine (GEE). Google Earth Engine provides a significant advantage for geospatial research considering its vast storage of earth observing satellite data, robust tools for remote sensing analysis, and ease of access for research use. We used the GEE platform to analyze all the available Copernicus Sentinel-2 imagery to amass a high

Figure 14 Comparison of true colour satellite imagery, Minas Basin. A) Low tide Landsat Oct. 5, 1996. B) Low tide Sentinel-2 July 8, 2019. C) High tide Sentinel-2 August 7, 2017. D) Low tide with salt marsh Sentinel-2 August 2, 2017.

resolution (10 meter) layer depicting the extent of the intertidal zone seamlessly (Fitton et al., 2021). This calculation is done by computing a simple water mask pixel-by-pixel for each individual image and then calculating a complete 'percent of time underwater' across all images. This simple metric is this used to identify 10x10 meter pixels of intertidally exposed bedrock and mudflat where water is observed to inundate only in 70 and 95% of the images (Figure 15). Using the GEE platform, this computation has been completed using all available Sentinel-2 images captured across the inner bay ranging from March 2017 to December 2021 incorporating as many as 880 images for a given location, and a total of 6601 images across the wider region. Additionally, intertidal vegetation and marsh lands were mapped using a similar technique and an appropriate 'vegetation mask'. These data were compared against high precision lidar and the modelled HHWLT to derive the extent of existing mudflats and salt marsh communities in the region. This approach may prove to be an invaluable tool for providing insights for conservation planning due to its robustness, simplicity, and repeatability.

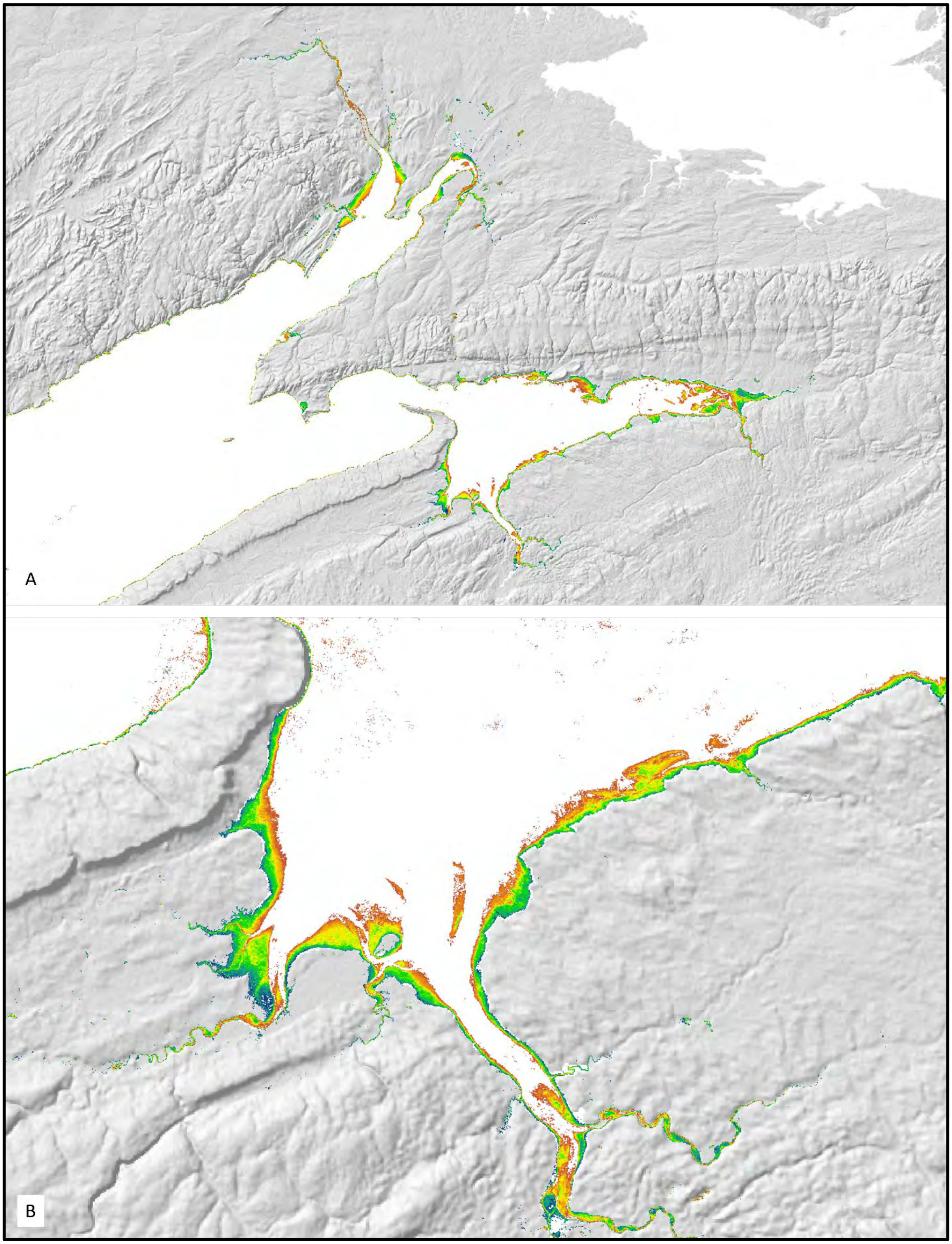

Figure 15 Example initial output from GEE. A) Map of IBoF showing pixel count of how long an area is out of water. B) Close up of Minas Basin coast with exposure pixel count.

As mentioned, once the intertidal areas were mapped, a vegetation mask was then applied. This was based on the concept of a Normalized Difference Vegetation Index (NDVI) which uses the rand ratio combinations of red and near-infrared. The initial data processing highlighted all vegetated areas both in the intertidal zone and landward of dykes within the extent of the HHWLT range discussed earlier (Figure 16). These data were further refined, and a salt marsh layer was produced

Figure 16 Example of vegetation within the intertidal zone and the extent of HHWLT landward of the dykes near Windsor, NS.

that consisted of low marsh and high marsh vegetation species as well as a mudflat layer (Figure 17). These layers represent the extent of mudflat, and salt marsh post dyke construction. There was some confusion between salt marsh vegetation that grows on mudflats and rockweed that grows on bedrock outcrop and boulders. We visually compared the slat marsh layers to high-resolution orthophotos to select and change the salt marsh to rockweed where we interpreted it to be growing. The extent of the mudflat is controlled in large part to the tidal range, coastal elevation, and sediment supply. To estimate the extent of what mudflats could have existed if no dykes were built in the IBoF, we can use the full extent of the HHWLT range as an estimate for the possible extent of tidal flats as depicted on Figure 7.

Figure 17 Example of Salt Marsh (low and high) and mudflat layer for Minas Basin area.

In order to calculate the possible extent of low marsh and high marsh if there were no dykes, we calculated the elevation statistics of the marsh types for each of the five regions previously discussed. The occurrence of low and high salt marsh vegetation is dependent on their tidal exposure and substrate (Figure 18). To calculate the possible extent of low marsh and high marsh if there were no dykes holding back the tides, elevation statistics were generated from the lidar DEMs for the low and high marsh areas of the five regions. This involved using the low and high salt marsh polygons and generating elevation statistics from the lidar DEM (Figure 19). The mean elevation plus and minus one standard deviation was used for each of the five regions to then applied to the lidar DEM to calculate where these salt marsh communities could grow if there were no dykes. Care was taken to ensure the marsh elevation thresholds did not exceed the maximum elevation of the HHWLT.

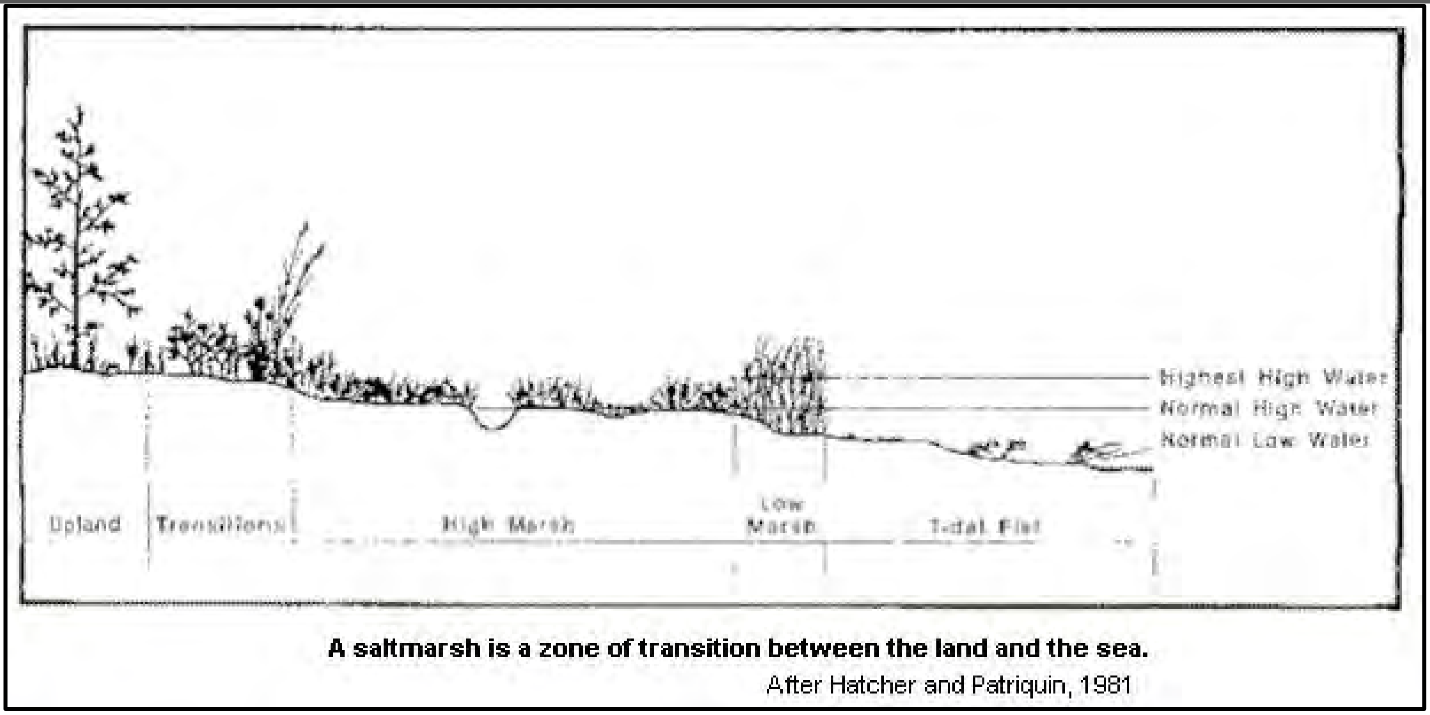

Figure 18 Cartoon of the relationship between elevation/tidal exposure and low and high marsh communities.

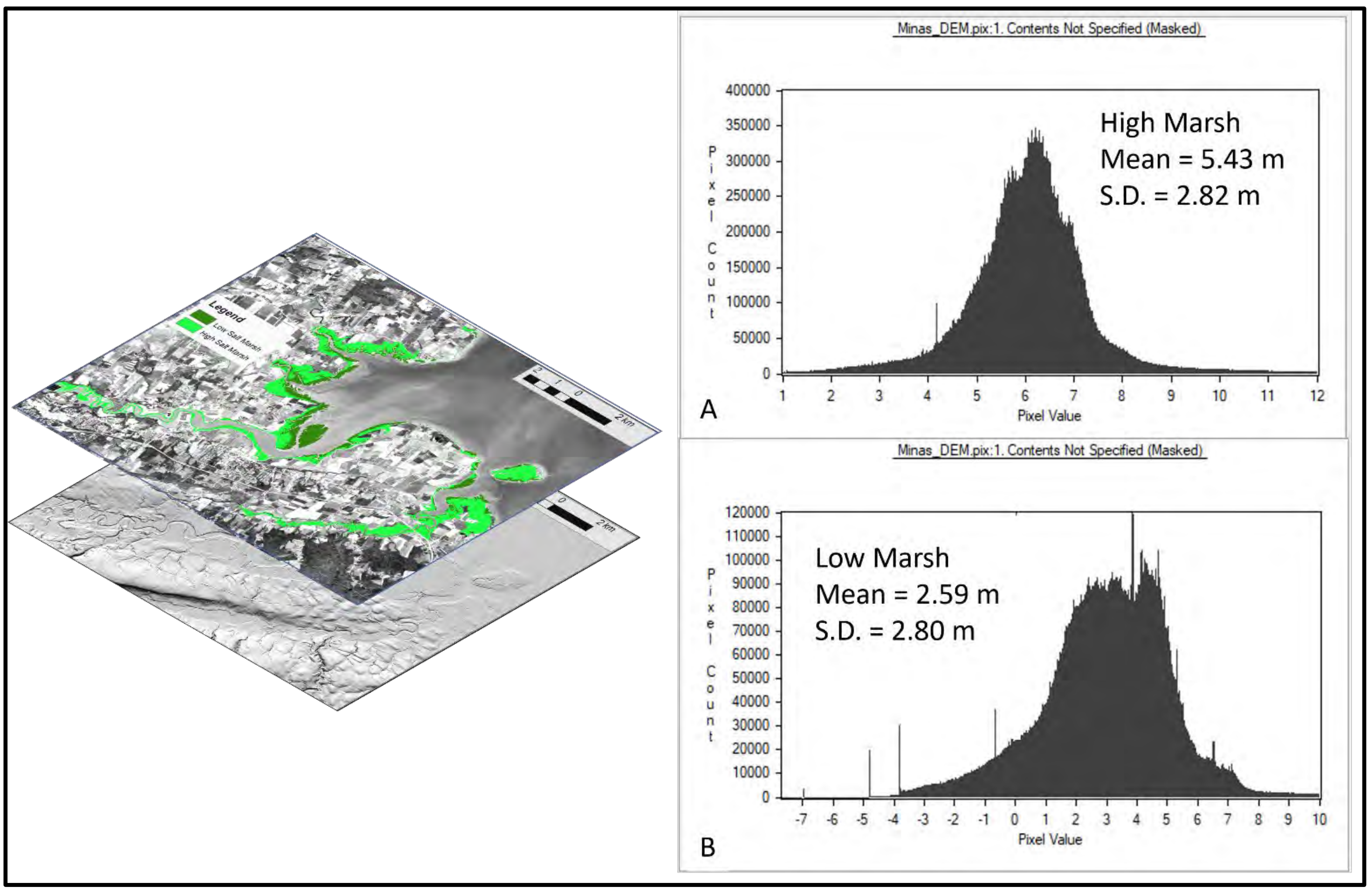

Figure 19 Example of how the elevation statistics were generated for low and high salt marsh areas. Left images show the salt marsh polygons with the lidar elevation under them. Right graphs show the elevation distribution and key statistics for high marsh (top) and low marsh (bottom) for the Minas Basin region.

The potential elevation range for the low and high salt marsh for the five regions were then applied to the lidar DEM to map the possible extent for the marshes up to the maximum HHWLT boundary. The elevation range threshold minimum and maximum used with the lidar to map low and high salt marsh are depicted in Table 3. Note that the NS Coast and NB Coast were not included in this table as these areas are dominated by bedrock outcrop and the occurrence of rockweed rather than salt marsh. Also, in most cases the upper threshold of the low marsh (mean + 1 STD) overlapped with the lower threshold of the high marsh (mean – 1 STD). In these cases, we took the midpoint between these two thresholds to represent the upper threshold of the low marsh and the lower threshold of the high marsh (Table 3).

Region	Marsh Type	Mean Elevation	STD Elevation	Elevation Range Min.	Elevation Range Max.
Chignecto	High	5.90	2.03	5.82	6.40
Chignecto	Low	4.38	3.36	1.02	5.82
Cobequid	High	7.20	2.41	6.23	7.50
Cobequid	Low	4.49	3.17	1.32	6.23
Minas	High	5.43	2.82	4.00	7.20
Minas	Low	2.59	2.80	-0.21	4.00

Table 3 Table of elevation threshold values used to map potential low and high salt marsh areas landward of dykes.

2.2 Key Ecological Attributes and Associated Target Health and Threat Indicators

Multiple publicly available layers were used to create the threat/disturbance layer (Table 4). Many of these features were buffered and used for proximity analysis with other natural features: beaches, coastal islands, mudflats and salt marshes.

Layer	Source
NS Buildings	NS Geographic Data Directory
NB Buildings	GeoNB
NS Dams	CanVec Manmade Features
NB Dams	CanVec Manmade Features
NS Breakwaters and Dykes	CanVec Manmade Features
NB Breakwaters and Dykes	CanVec Manmade Features
NS Marine Aquaculture Sites	NS Geographic Data Directory
Ferry Routes	Government of Canada Open Data
NS Rockweed Leases	NS Geographic Data Directory
NS Roads	NS Geographic Data Directory
NB Roads	GeoNB

Table 4 List of GIS layers that were used in the threat spatial analysis.

The GIS threat layers were merged buffered by 100 m. The watershed extents draining into the IBoF were used as the cut-off boundary for threats. An example of the 100 m buffer for the roads, buildings and dykes for Chignecto is presented (Figure 20).

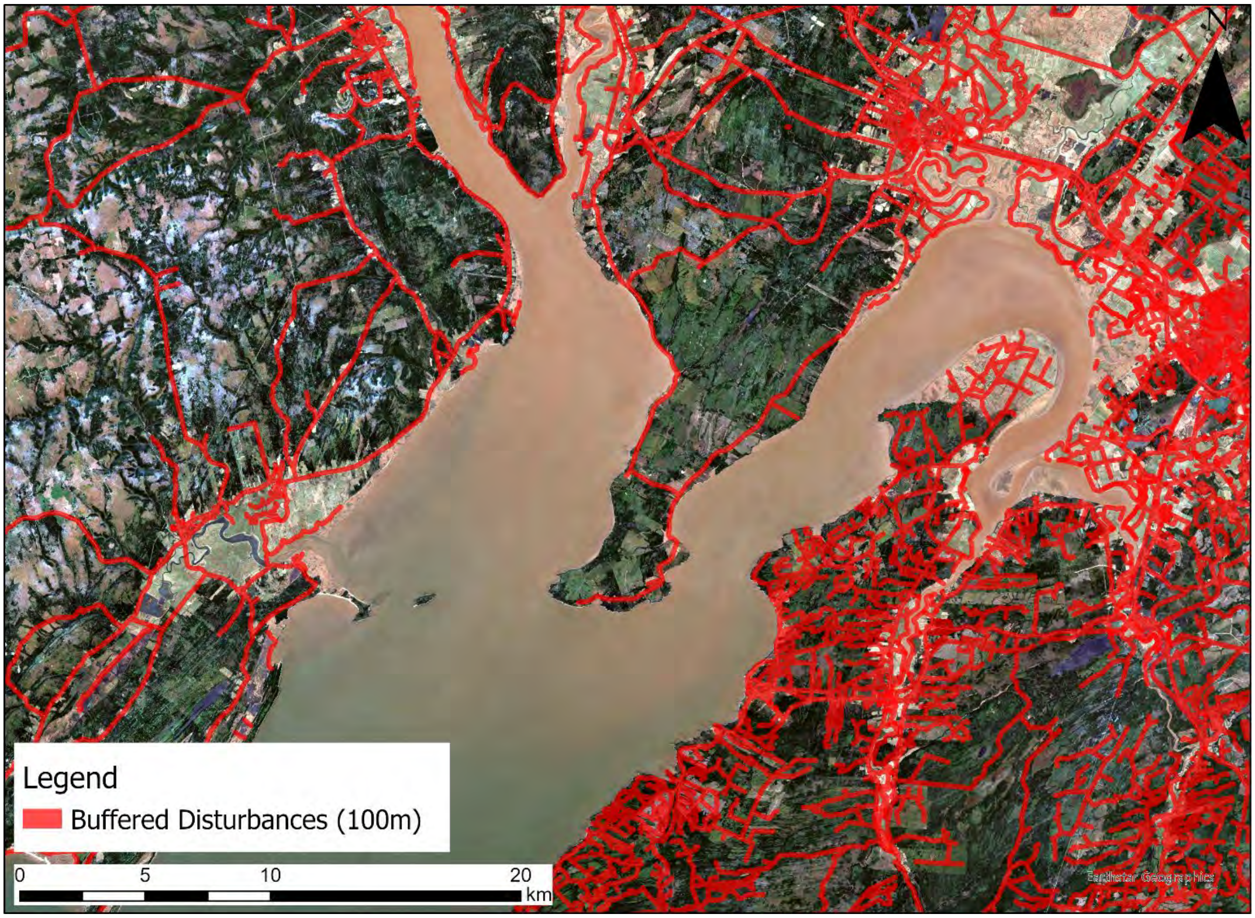

Figure 20 Example of 100 m buffer calculated for the road network, buildings and dykes in Chignecto Basin.

An island GIS layer was constructed using a combination of provincial vector mapping and the lidar DEM. The islands were buffered by 100 m to assess the threats (Figure 21). As only the land-based threats were being considered for the islands, the buffer was then clipped to the extent of the mainland and intersected with the threat buffer covering to indicate where they overlapped (Figure 21).

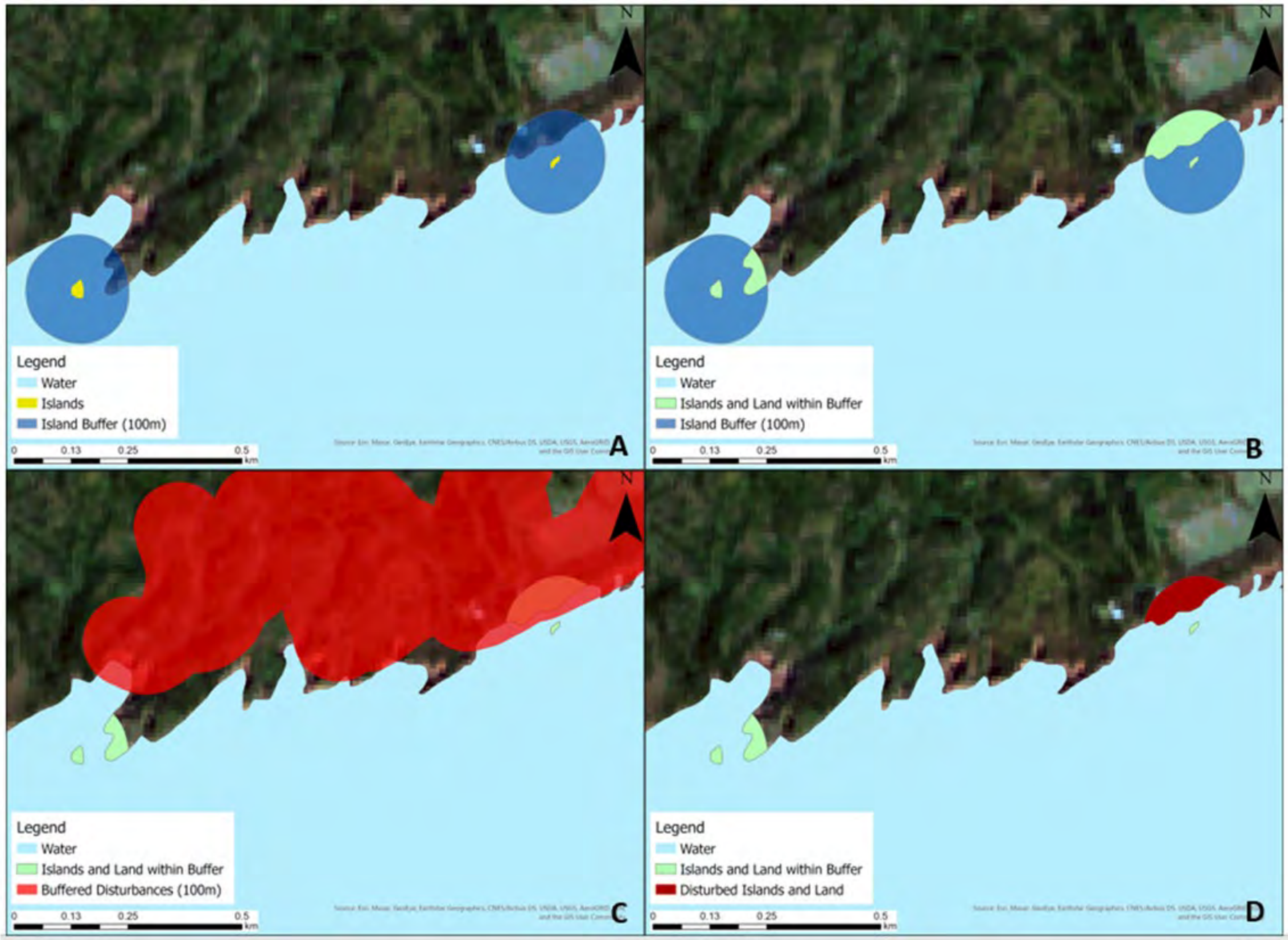

Figure 21 Example of buffer analysis for islands and terrestrial threats. A) 100 m buffer of islands (blue). B) 100 m buffer of islands on land (green). C) Terrestrial threat 100 m buffer (red). D) Threat 100 m buffer intersected with 100 m island buffer (red polygon).

Beaches were constructed from Environment and Climate Change Canada's Atlantic Shoreline Classification layer available from the Government of Canada's Open Government data website. The ECCC Shoreline layer is classified into 10 categories: Marsh, Mud Tidal Flat, Sand Tidal Flat, Man-Made Solid, Bedrock Platform, Bedrock Cliff / Vertical, Sand Beach or Bank, Boulder Beach or Bank, Mixed Sediment Beach or Bank, and Pebble / Cobble Beach or Bank. The four Beach or Bank categories were used to build the beach GIS layer (Figure 22).

Cliffs were constructed from Natural Resources Canada CanCoast Version 5.0 layer available from the Government of Canada's Open Government data website. CanCoast is a collection of datasets that describe the physical characteristics of Canada's marine coasts. It includes datasets that are not expected to change through time (such as coastal materials and backshore slope), and some that are projected to change as climate changes (such as wave height and mean sea level). The Backshore Slope attributes was used to map cliffs. The CanCoast layer slope attribute is categorized in (Table 5).

Slope Score	Slope Degree
1	25+
2	16-24
3	6-12
4	2-5
5	0-1

Table 5 NRCan CanCoast GIS layer with slope classification.

Line segments with scores ranging from 1-2 were used for the construct the Cliff GIS layer (Figure 22). Both the cliffs and beaches layers were buffered by 100 m and intersected with the buffered disturbance layer to assess disturbance level.

Figure 22 Example of beaches and derived cliffs. Beaches were extracted from the ECCC shoreline classification and cliffs from CanCoast utilizing the slope attribute.

With regards to marine activity in the IBoF, lobster fishing areas 27 – 38 Integrated Fisheries Management Plan (DFO 2020) outlines the boundaries for lobster fishing areas (LFAs) in Nova Scotia and New Brunswick. As the entirety of the study area was encapsulated in LFAs 35 and 36, a water polygon for the inner Bay of Fundy was used as the Lobster Fishing Area threat polygon (Figure 23). The Lobster Fishing Area was not included in the merged threats, as LFAs are only relevant to the Marine Health Surrounding Island's KEA.

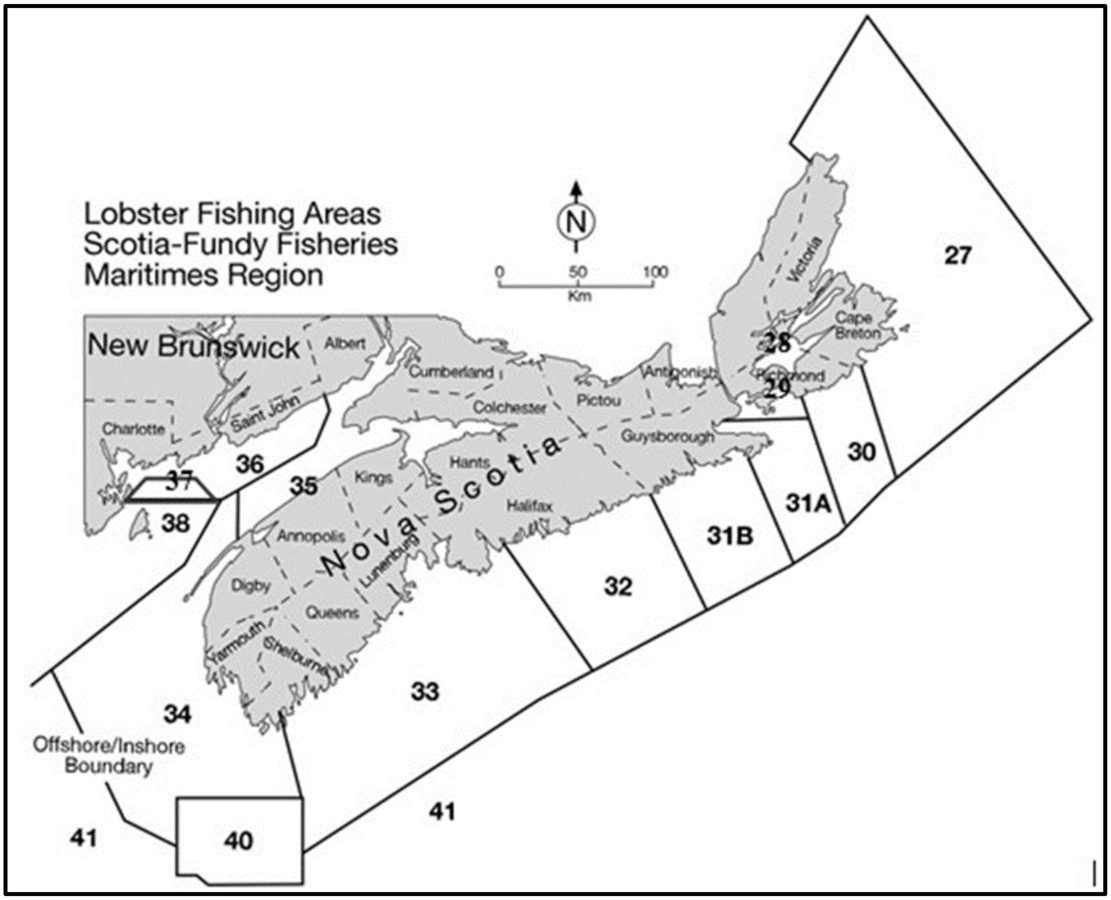

Figure 23 Lobster Fishing Areas 27 – 38 Integrated Fisheries Management Plan, DFO 2020. The IBoF is covered by sectors 35 and 36.

2.3 Watersheds draining into the IBoF

Watersheds from NS and NB were downloaded from their geospatial portals and those draining into the IBoF extracted and were included in the geodatabase (Figure 24). We have also included an impervious surface layer that was constructed for the ECCC Dartmouth office in 2014 utilizing Landsat imagery. The impervious surface layer represents the percentage (0-100) of impervious surface material per 30 m pixel. The insets on figure 24 show the communities of Moncton, Amherst and Truro that have the larges amount of impervious surface material in the watersheds draining into the IBoF. Saint John, NB is not part of the IBoF as defined in this project but is has a significant amount of impervious surface material that is just outside the study area (Figure 24). The amount of impervious surface material effects the flood risk in the area as it prevents infiltration of water into the ground and promotes runoff which can include contaminants which are detrimental to the coastal and marine ecosystems.

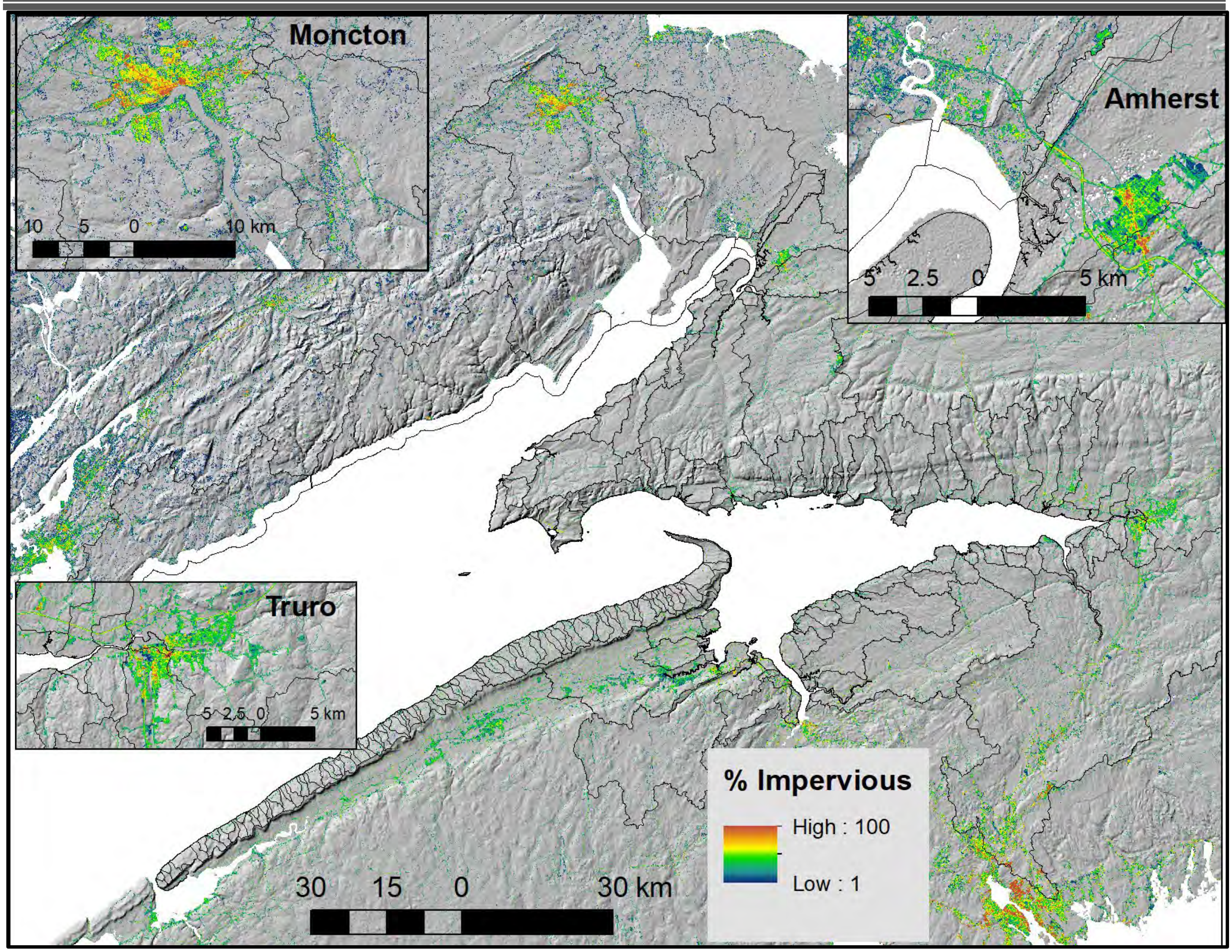

Figure 24 Watersheds draining into the IBoF (black lines) with shaded relief SRTM DEM and impervious surfaces.

2.4 Construction of a Seamless DEM for IBoF

A seamless 10 m DEM was constructed from a variety of sources including the provincial NS and NB lidar along the coast, Shuttle Radar Topography Mission (SRTM) data and chart soundings. The 1 m lidar data were resampled to 10 m and the SRTM data was resampled from 30 m to 10 m and the soundings were point data that were interpolated. A 10 m bathymetric grid derived from various multibeam surveys conducted by CHS and NRCan also exists for part of the IBoF. The various data were interpolated and at the location of adjoining datasets, the data were blended using an inverse distance weighting function to smooth any discontinuities between datasets.

3 Results

The various GIS and image processing analysis has resulted in the construction of many new GIS layers for the IBoF. topo-bathymetric lidar survey for the Stewiacke River are impressive, given the size and length of the area surveyed and the challenging environmental conditions that were occurring during the survey period. As mentioned, the study area is quite large and has a convoluted shape, thus the orthophoto maps were broken into four sections to facilitate quicker access and loading of the imagery in GIS (Figure 15).

3.1 IBoF Shoreline today and in 2100

The present-day shoreline as defined by NS and NB represents the mean high waterline as defined visually and is not associated with a specific elevation. For this project we utilized the coastal lidar and the elevation of HHWLT to define the shoreline today. We used the RSL and added it to the HHWLT to predict where the shoreline would be in 2100 (Table 6).

Region	Present-day HHWLT (m CGVD2013)	RSL 2100 (Global SLR, crustal subsidence, tidal amplification, Western Antarctic Ice Sheet collapse	Shoreline 2100 (HHWLT + RSL) (m CGVD2013)
Cobequid	7.5	1.8	9.3
Minas	7.2	1.85	9.1
Chignecto	6.7	1.8	8.5
NB Coast	4.3	1.9	6.2
NS Coast	4.6	1.8	6.4

Table 6 Table of present day HHWLT and predicted HHWLT in 2100.

The present-day shoreline was presented in the methods (Figure 8) and the projected shoreline for 2100 considering RSL was presented in Figure 9.

3.2 Coastal Flooding today and in 2100

The present day and predicted flooding in 2100, considering dykes and other barriers, was modelled using the values in Table 1. The same water levels were used for modelling present day and 2100 flooding assuming no dykes (Figure 25). As noted in the figure, the maps are very similar irrespective if the dykes are considered or not. This is because the water level considered (HHWLT plus 100-year return period storm surge) exceed the dykes, therefore the extent of inundation is similar regardless of dyke consideration or not.

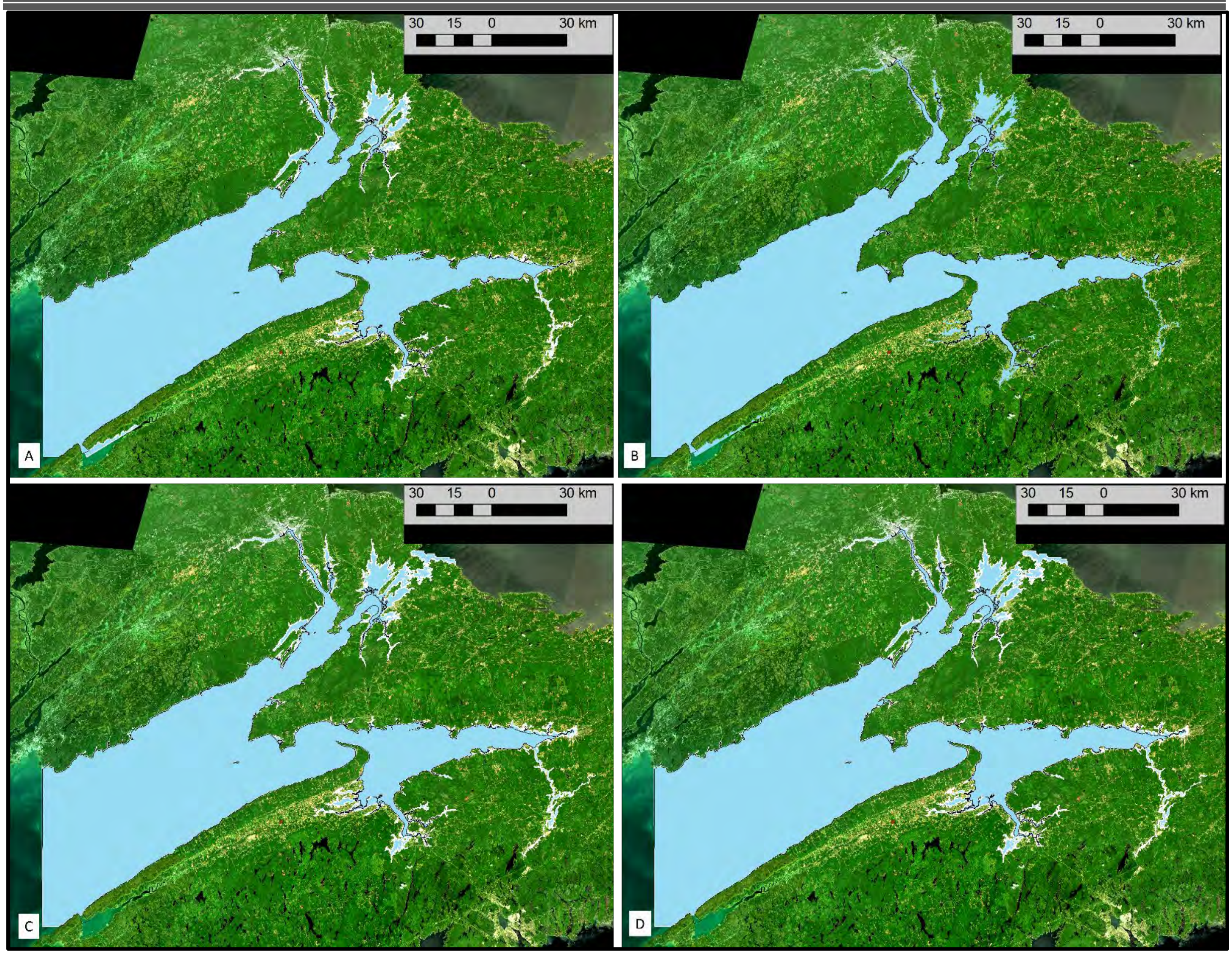

Figure 25 Coastal flood risk today and in 2100. A) Present-day flood risk considering dykes. B) A) Present-day flood risk considering no dykes. C) Flood risk in 2100 considering dykes. D) Flood risk in 2100 flood risk considering no dykes.

3.3 Head of Tide for Major Rivers in IBOF

The head of tide as calculated for each of the 48 rivers identified as flowing into the IBoF (Table 2). As mentioned in the methods care was taken to examine various image datasets, including Google Street View to determine if a barrier was present that could limit the head of tide extent. Figure 26 shows an example of the Chiganois River where an aboiteau limits the head of tide extent. Table 7 shows a list of 13 rivers that have control structures near their mouth.

River Name
Shepody River (NB)
Memramcook River (NB)
Carters Brook (NB)
Tantramar River (NB)
Aulac River (NB)
Missaguash River (NS)
LaPlanche River (NS)
Nappan River (NS)
Habitant River (NS)
St. Croix River (NS)
Tennycape River (NS)
Great Village River (NS)
Chiganois River (NS)

Table 7 List of rivers with control structures at their mouth.

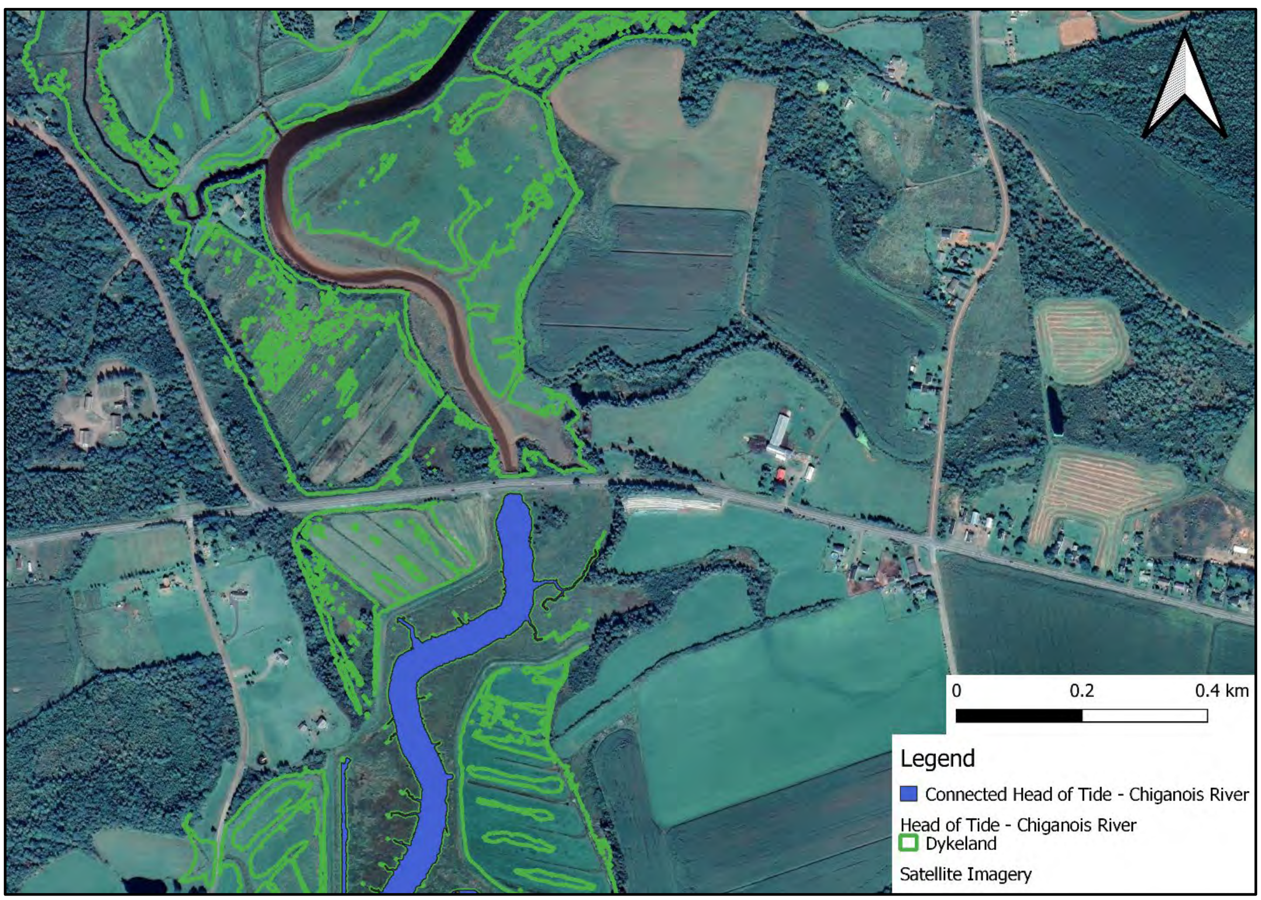

Figure 26 Example of a barrier (aboideaux) at Chiganois River that limits the head of tide for this river.

3.4 Mapping Tidal Flats & Salt Marsh with Pre and Post Dykes

The mudflats and salt marsh data were derived from Google Earth Engine but needed to be manually refined and edited. The intertidal mudflats were generated based on examining a series of Sentinel-2 images to determine how often then were inundated. This produced an intertidal map that did not differentiate between mudflat and bedrock outcrop. This was manually edited to remove the bedrock features (Figure 27).

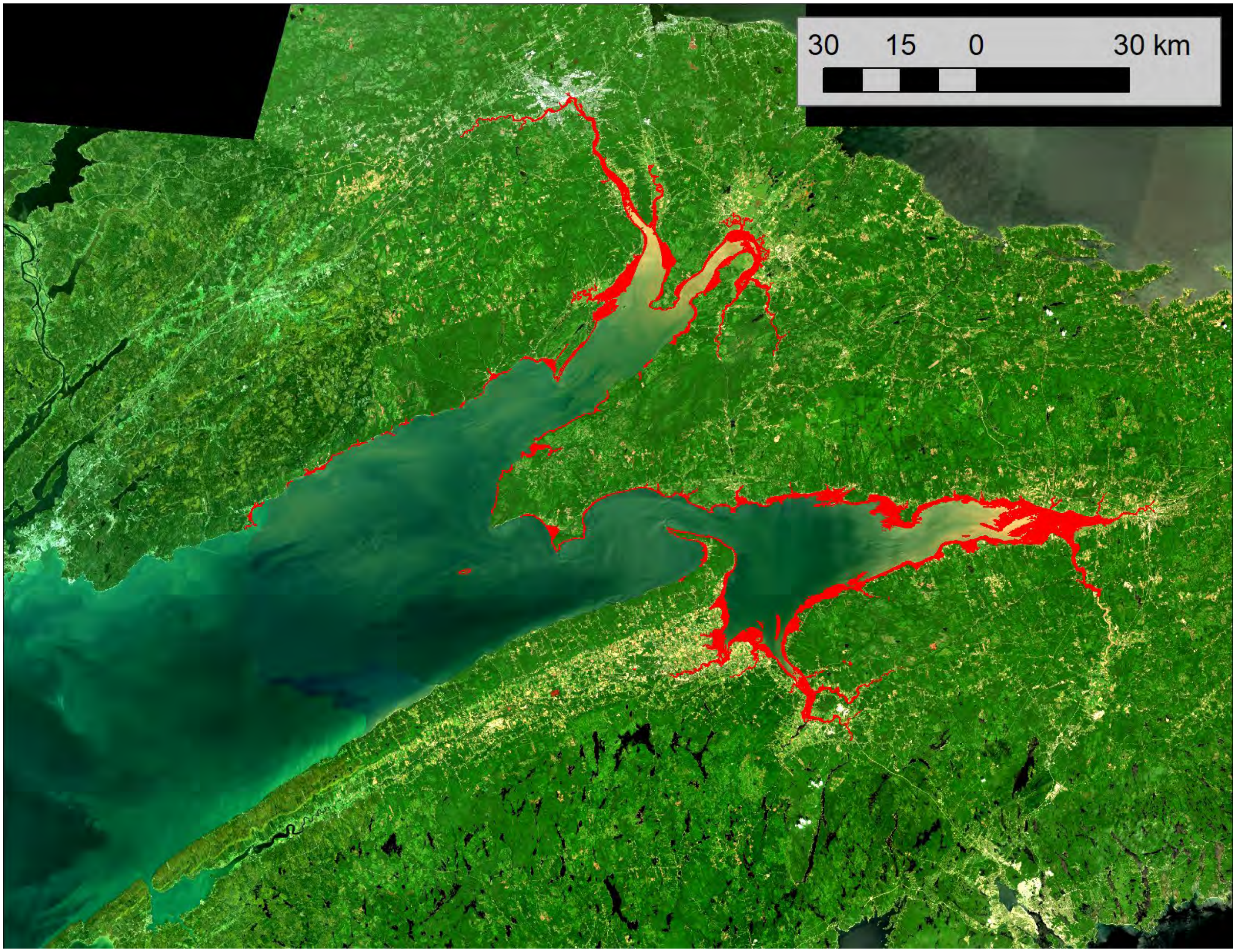

Figure 27 Present day distribution of intertidal mudflats.

In order to generate the extent of mudflats if there were no dykes, we assume everything landward of the dykes and less than the HHWLT would become mudflat. To achieve this the HHWLT polygon that is not connected to the ocean was used in combination with the present-day mudflats to calculate the possible extent of mudflats pre dyke construction (Figure 28).

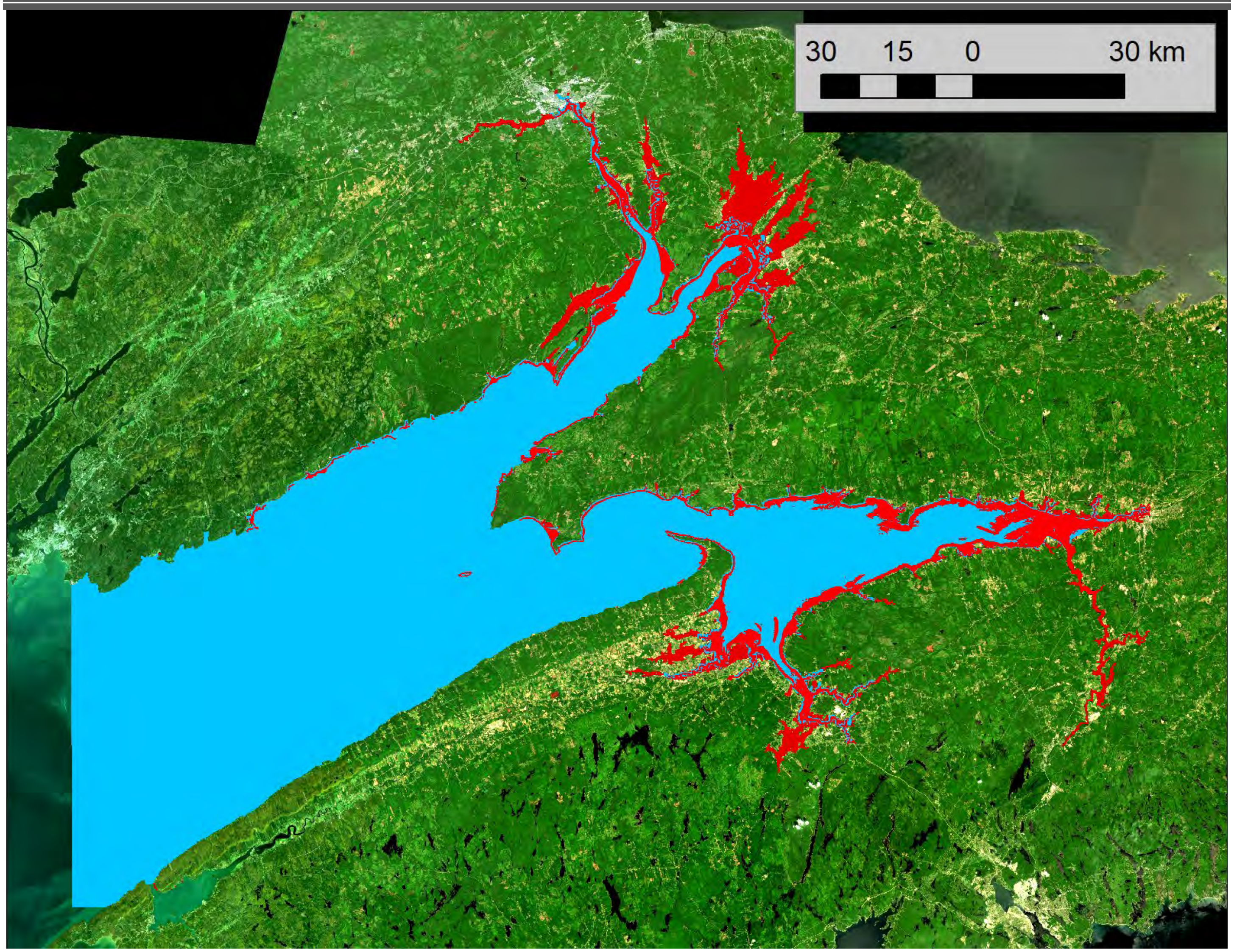

Figure 28 Modelled extent of mudflats (red) if no dykes were built.

The salt marshes were extracted in a similar fashion as the mudflat, but an extra criterion was applied to differentiate vegetated and no-vegetated intertidal areas. Unfortunately, this did not differentiate salt marsh vegetation from rockweed, thus the layer had to be inspected and manually edited to ensure just salt marsh was included. Once the saltmarsh layer was refined, it was used to separated low marsh from high marsh based on the Normalized Difference Vegetation Index (NDVI= (NIR-R)/(NIR+R) values derived from the Sentinel-2 imagery. The individual Sentinel-2 images Figure 14-D were used as a guide to differentiate low marsh from high marsh vegetation. Once the low and high marsh were separated the elevation statistics for each were extracted from the lidar DEM and thresholds defined as outlines in Table 3 to calculate where low and high marsh may grow if no dykes were built. The result of this analysis shows that several low-lying areas landward of the dykes appear suitable (elevation wise) for the formation of salt marsh (Figure 29). Similar analysis was carries out with projecting the mudflats and salt marshes if no dykes were present. The constraints applied include the mudflats must be within the boundary of HHWLT and the elevation thresholds were used to model potential low and high salt marsh areas if no dykes were present (Figure 29).

Figure 29 Minas Basin low and high salt marsh post and pre-dyke construction. A) Present-day salt marsh. B) If no dykes were built where salt marsh could grow.

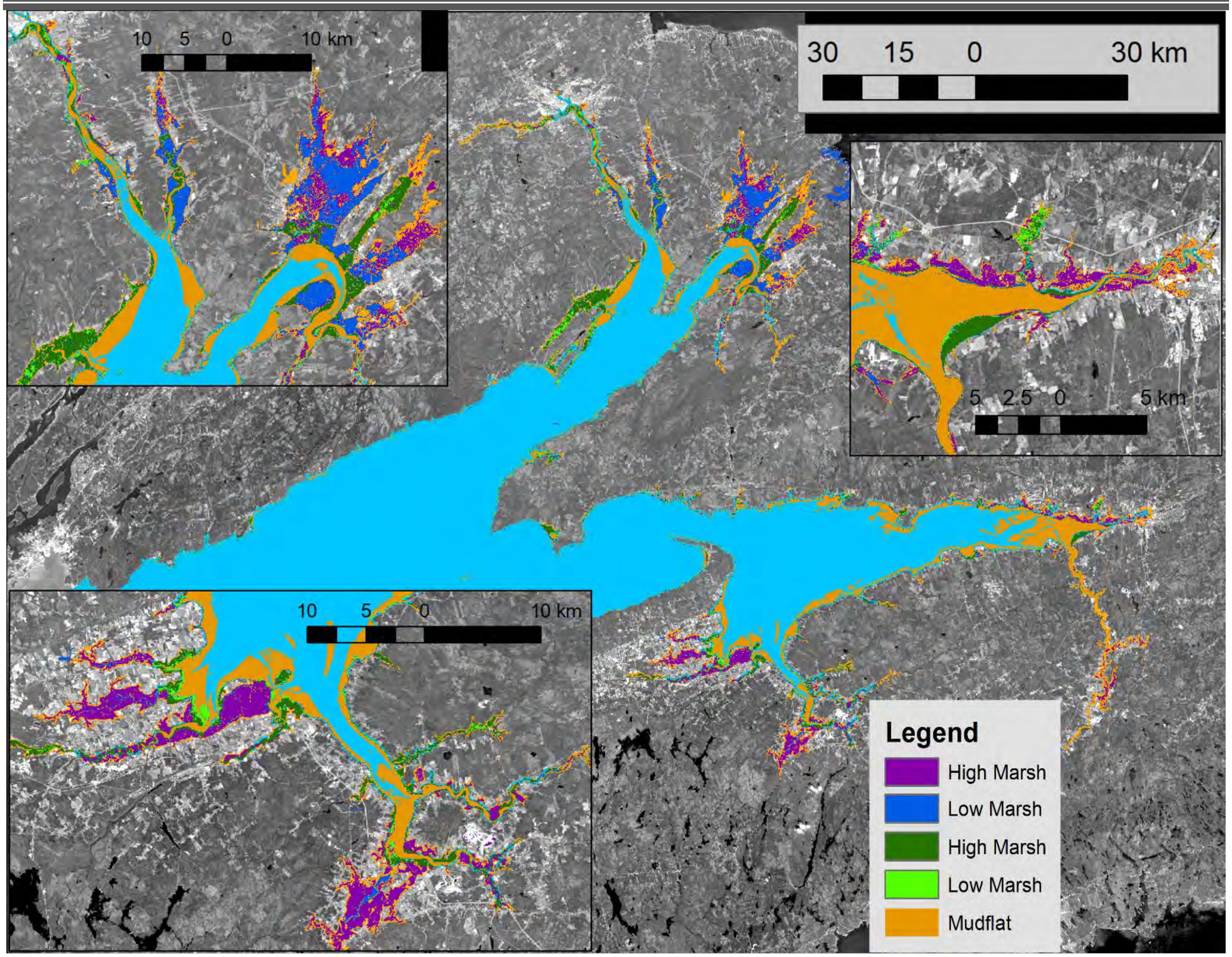

Figure 30 Present day low and high marsh (greens) and mudflats (brown) and modelled potential mudflats (brown) and low marsh (blue) and high marsh (purple). Inset maps top left (Chignecto), top right (Truro), bottom left (Minas Basin).

The area of these various layers, existing mudflat and salt marsh and modelled mudflat and slat marsh will be calculated once these layers have been reviewed by the IBoF team and accepted.

Preliminary analysis of the tidal mudflats indicates that prior to the dykes being built there was the potential for 69,18 ha of mudflat, this does not consider how much of this area could have support salt marsh as reported below. This area includes all the existing mudflat seaward of the dykes and the potential area landward of the dykes up to the HHWLT elevation. After the dykes were built, the present-day extent of the mudflats is 42,093. This represents a loss of 39.5% (Table 8).

Total Pre Dyke Mudflat	Total Post Dyke Mudflat	% Loss Mudflat
69,618 ha	42,093 ha	39.5 %

Table 8 Area of mudflat pre and post dyke construction.

Preliminary analysis indicates there is 42,093 ha of current mudflats of which 2016 are withing the 100 m disturbance buffer or approximately 4.8%.

Preliminary analysis indicates that the total salt marsh we have lost approximately 66% from the time before dykes were built, a loss of ~30,000 ha.

Total Pre Dyke Salt Marsh	Total Post Dyke Salt Marsh
44,889 ha	15,066 ha

Table 9 Area of salt marsh pre and post dyke construction.

Much of the loss appears to be related to the low marsh category where 85% has been lost while the high marsh has been diminished by 45%.

	Pre Dyke Low Marsh	Pre Dyke High Marsh	Post Dyke Low Marsh	Post Dyke High Marsh
	23,591 ha	21,297 ha	3,443 ha	11,623 ha

Table 10 Area of low and high salt marsh pre and post dyke construction.

3.5 Key Ecological Attributes and Associated Target Health and Threat Indicators

The total number of islands within the IBoF is 153. The extent of islands and land within a 100 m of disturbance is 723 ha with 37 islands being within the 100 m disturbance buffer, or 24% and 76% undisturbed. We calculated there are 202 beaches forming a linear extent of 594 km. Of these beaches, 148 are within the 100 m disturbance buffer or 74% of the beaches disturbed. The linear length of disturbed beaches is 486 km or 82% of the beach length is disturbed.

3.6 Construction of a Seamless DEM for IBoF

The seamless DEM was constructed from three main sources: 1) chart soundings, 2) coastal topographic lidar, and 3) SRTM elevation inland. Seamless DEM 10 m was gridded at resolution and the elevations are references to CGVD2013. The data have been coloured and shaded to form a colour shaded relief map (Figure 31).

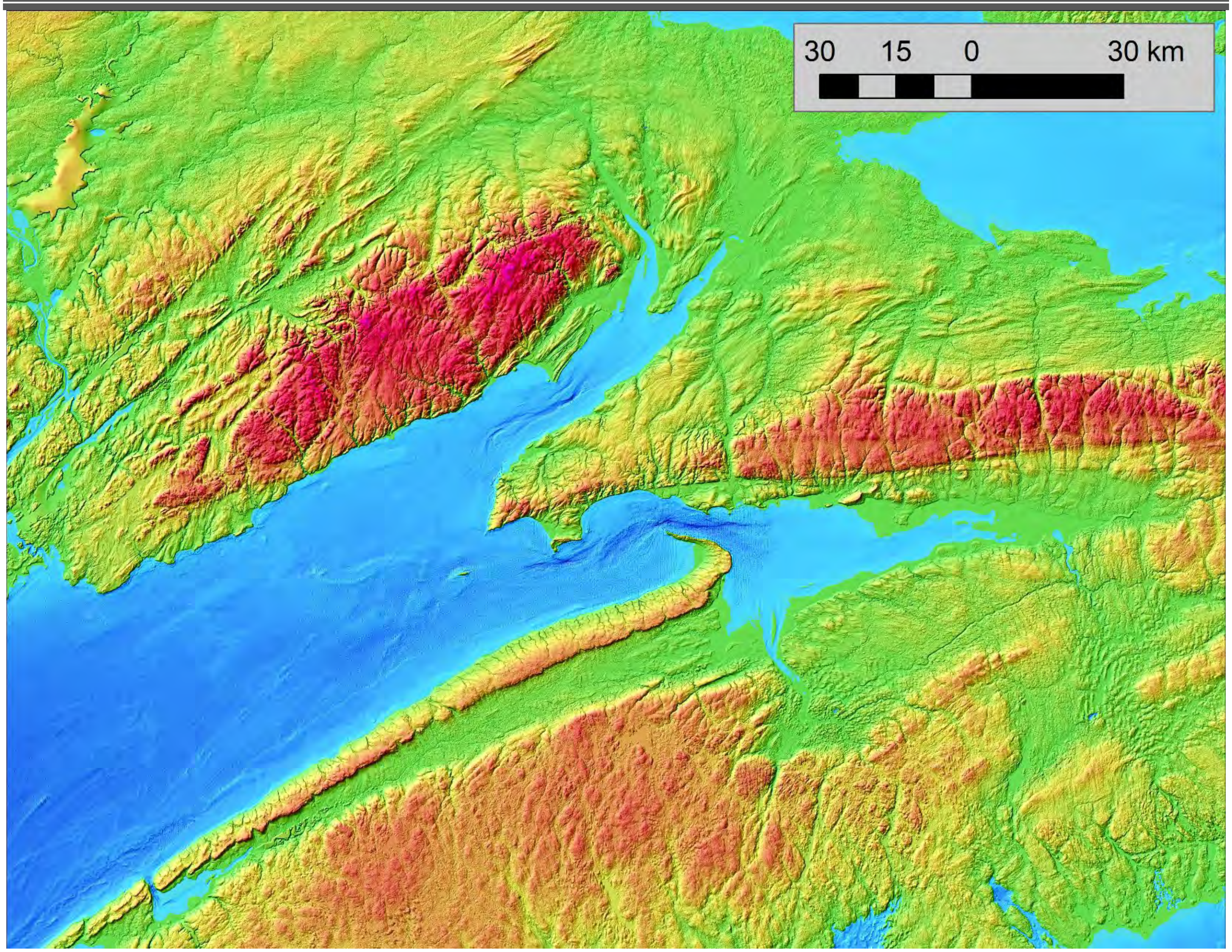

Figure 31. Seamless elevation model of the IBoF. Data sources include: chart soundings, coastal topographic lidar, SRTM elevation inland. Seamless DEM 10 m resolution, elevations CGVD2013.

4 Conclusion

This project has presented some interesting challenges to develop layers that did not exist prior to this study. The HHWLT information from CHS-DFO provided the basis for much of the analysis and landward limits of the data. The HHWLT was used to calculate the extent of the head of tide for 48 rivers draining into the IBoF. It was also used in addition to the 1 in 100-year storm surge event height to calculate the present-day flood risk and considering climate change and RSL the flood risk in 2100. Since the HHWLT varied considerably throughout the study area the flood risk analysis, which was based on the GIS bath tub model approach, had to be split up into five regions based on the HHWLT range. The flood layers were then recombined for the entire bay from these five regions. The extent of mudflats and salt marshes were extracted from a time-series of Sentinel-2 images through Google Earth Engine. The exposure above water was used to map the mudflat extent and NDVI was calculated to map vegetated areas within this zone. The salt marshes were then separated into low and high marsh based on their NDVI values. The existing areas of mudflat and salt marsh were calculated. The amount of mudflat that could have existed before the dykes were built was estimated by calculating the area landward of the dykes that was connected and below the HHWLT elevation. For the salt marshes, elevation statistics were calculated for the low and high marsh for each of the 5 regions from the lidar DEMs. The mean plus and minus 1 standard deviation was used to calculate elevation thresholds for the low and high marsh, which were modified to ensure no overlap between boundaries and did not exceed the HHWLT elevation. The lidar data landward of the dykes were then modelled based on these salt marsh elevation threshold values to predict where low and high marsh could grow. Analyses indicates that approximately 40% of mudflat and 66% of salt marsh have been lost as a result of dyking. Several threats, including roads, building and dykes were used to construct buffers to test how much of the mudflats, salt marshes and islands were within this disturbed zone. The analysis conducted during this phase of the project will be reviewed and possibly refined during phase 2 of the project.

5 References

Fitton, J. M., Rennie, A. F., Hansom, J. D., & Muir, F. M. E. 2021. Remotely sensed mapping of the intertidal zone: A Sentinel-2 and Google Earth Engine methodology. Remote Sensing Applications: Society and Environment, 22, 100499. doi:10.1016/j.rsase.2021.100499.

Greenberg, D.A., Blanchard, W., Smith, B., E. Barrow. 2012. Climate Change, Mean Sea Level and High Tides in the Bay of Fundy, *Atmosphere-Ocean*, DOI: 10.1080/07055900.2012.668670.

Hatcher, A. and Patriquin, D.G (eds.). 1981. Salt marshes in Nova Scotia: a status report of the Saltmarsh Working Group. Halifax: Institute of Resource and Environmental Studies and Department of Biology, Dalhousie University, 70 pp.

IPCC 2013: Summary for Policy makers. In: Climate Change 2013: The Physical Science Basis. Contribution of Working Group I to the Fifth Assessment Report of the Intergovernmental Panel on Climate Change. Eds Stocker, T.F; Qin, D.; Plattner, G.K; Tignor, M; Allen, S.K; Boschung, J; Nauels, A; Xia, Y; Bex, V; and P.M. Midgley.

James, T.S., Henton, J.A., Leonard, L.J., Darlington, A., Forbes, D.L., and Craymer, M. 2014. Relative Sea-level Projections in Canada and the Adjacent Mainland United States; Geological Survey of Canada, Open File 7737, 72 pp. doi:10.4095/295574

Richards, R. and R., Daigle. 2011. Scenarios and Guidance for Adaptation to Climate Change and Sea-Level-Rise - NS and PEI Municipalities.

van Proosdij, D.; Ross, C. and G., Matheson. 2018. Risk Proofing Nova Scotia Agriculture: Nova Scotia Dyke Vulnerability Assessment. Submitted to NS Federation of Agriculture, 202 pp.

6 Appendix 1

As described in the methods, the HHWLT represents the 19-year average of the highest tides each year. To understand the relationship of HHWLT to the regular predicted tide, we downloaded the predicted tide for Burntcoat Head, Hantsport and Amherst point to compare elevations.

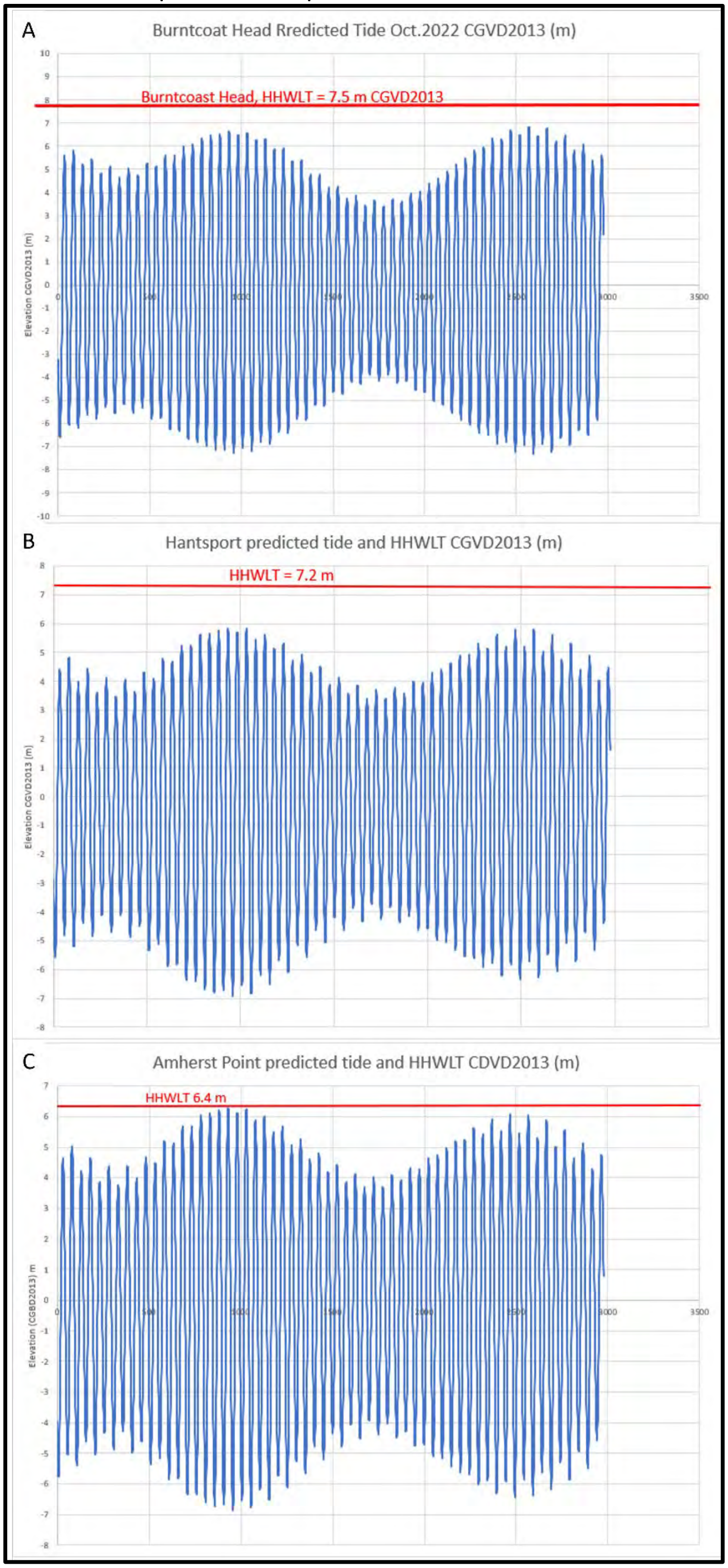

Figure 32 Comparison of predicted tide (Oct 2022) with HHWLT for Burtncoat Head, Hantsport and Amherst Point.